DYNAMIC ANALYSIS OF A CAROUSEL REMOTELY PILOTED VEHICLE RECOVERY SYSTEM

Russell Norman Robinson

DUDLEY KNOX LIBRARY
NAVAL POSTGRADUATE SCHOOL
MONTEREY, CA 93940

NAVAL POSTGRADUATE SCHOOL
Monterey, California

THESIS

DYNAMIC ANALYSIS OF A CAROUSEL

REMOTELY PILOTED VEHICLE RECOVERY

SYSTEM

by

Russell N. Robinson

December 1977

Thesis Advisor: L. V. Schmidt

Approved for public release; distribution unlimited.

T182109

DUDLEY KNOX LIBRARY
NAVAL POSTGRADUATE SCHOOL
MONTEREY, CA 93940

SECURITY CLASSIFICATION OF THIS PAGE (When Data Entered)

REPORT DOCUMENTATION PAGE

READ INSTRUCTIONS BEFORE COMPLETING FORM

1. REPORT NUMBER

2. GOVT ACCESSION NO.

3. RECIPIENT'S CATALOG NUMBER

4. TITLE (and Subtitle)
Dynamic Analysis of a Carousel Remotely Piloted Vehicle Recovery System

5. TYPE OF REPORT & PERIOD COVERED
Master's Thesis
December 1977

6. PERFORMING ORG. REPORT NUMBER

7. AUTHOR(s)
Russell N. Robinson

8. CONTRACT OR GRANT NUMBER(s)

9. PERFORMING ORGANIZATION NAME AND ADDRESS
Naval Postgraduate School
Monterey, California 93940

10. PROGRAM ELEMENT, PROJECT, TASK AREA & WORK UNIT NUMBERS

11. CONTROLLING OFFICE NAME AND ADDRESS
Naval Postgraduate School
Monterey, California 93940

12. REPORT DATE
December 1977

13. NUMBER OF PAGES
68

14. MONITORING AGENCY NAME & ADDRESS(if different from Controlling Office)
Naval Postgraduate School
Monterey, California 93940

15. SECURITY CLASS. (of this report)
Unclassified

15a. DECLASSIFICATION/DOWNGRADING SCHEDULE

16. DISTRIBUTION STATEMENT (of this Report)
Approved for public release; distribution unlimited

17. DISTRIBUTION STATEMENT (of the abstract entered in Block 20, if different from Report)

18. SUPPLEMENTARY NOTES

19. KEY WORDS (Continue on reverse side if necessary and identify by block number)
Remotely Piloted Vehicle
RPV Recovery System
Dynamic Analysis
Equations of Motion
Dynamic Modeling

20. ABSTRACT (Continue on reverse side if necessary and identify by block number)

A Carousel Remotely Piloted Vehicle (RPV) Recovery System consists of a vertical mast which supports a horizontal member that is free to rotate. The approaching RPV is caught by vertical cables suspended from the horizontal member and the kinetic energy of the RPV is dissipated through the motion of the recovery system. This thesis presents a simplified dynamic analysis to describe the motion of an RPV after impact with a

DD FORM 1 JAN 73 1473 EDITION OF 1 NOV 65 IS OBSOLETE
S/N 0102-014-6601

SECURITY CLASSIFICATION OF THIS PAGE (When Data Entered)

recovery system simulating the carousel system. The equations of motion for the RPV were obtained from Lagrange's equations and modeled using the Continuous System Modeling Program on the IBM 360-67 computer at the W.R. Church Computer Center, NPS.The results showed that damping was required on motion of both the horizontal member and the suspended cables in order to prevent possible damage to the 150 pound RPV at an assumed 50 knot approach speed. A sensitivity analysis was performed by varying the system design parameters and the results are presented in the body of the thesis.

Approved for public release; distribution unlimited.

Dynamic Analysis of a Carousel Remotely Piloted Vehicle Recovery System

by

Russell Norman Robinson
Captain, U.S. Army
B.S., Engineering, Pennsylvania Military College, 1969

Submitted in partial fulfillment of the requirements for the degree of

MASTER OF SCIENCE IN AERONAUTICAL ENGINEERING

from the

NAVAL POSTGRADUATE SCHOOL
December 1977

ABSTRACT

A Carousel Remotely Piloted Vehicle (RPV) Recovery System consists of a vertical mast which supports a horizontal member that is free to rotate. The approaching RPV is caught by vertical cables suspended from the horizontal member and the kinetic energy of the RPV is dissipated through the motion of the recovery system. This thesis presents a simplified dynamic analysis to describe the motion of an RPV after impact with a recovery system simulating the carousel system. The equations of motion for the RPV were obtained from Lagrange's equations and modeled using the Continuous System Modeling Program on the IBM 360-67 computer at the W.R. Church Computer Center, NPS. The results showed that damping was required on motion of both the horizontal member and the suspended cables in order to prevent possible damage to the 150 pound RPV at an assumed 50 knot approach speed. A sensitivity analysis was performed by varying the system design parameters and the results are presented in the body of the thesis.

TABLE OF CONTENTS

I. INTRODUCTION ---------- 11

II. ANALYSIS ---------- 15

A. ASSUMPTIONS ---------- 15

B. OVERVIEW OF ANALYSIS ---------- 18

C. DETAILED ANALYSIS ---------- 19

1. Lagrange's Equation ---------- 19

2. Derivation of RPV Velocity ---------- 21

3. Derivation of Equations of Motion ----- 24

a. θ Equation of Motion ---------- 24

b. ϕ Equation of Motion ---------- 26

c. ψ Equation of Motion ---------- 28

4. Solving the Equations of Motion ------- 29

III. SYSTEM DESIGN ANALYSIS AND RESULTS ---------- 33

A. UNDAMPED SYSTEM ---------- 33

B. DAMPING ADDED TO HORIZONTAL MEMBER -------- 35

C. DAMPING ADDED TO RECOVERY ROD ---------- 36

D. IMPLEMENTING DAMPING ON A RECOVERY CABLE -- 54

IV. CONCLUSIONS AND RECOMMENDATIONS ---------- 60

APPENDIX ---------- 62

LIST OF REFERENCES ---------- 67

INITIAL DISTRIBUTION LIST ---------- 68

LIST OF TABLES

I. ϕ Variation for Undamped System ---------- 34

II. ϕ Variation with C_1 Damping ---------- 37

III. ϕ Variation with C_1, C_2 Damping ---------- 44

LIST OF FIGURES

1. Carousel Recovery System ---------- 13

2. Aquila Mini-RPV ---------- 14

3. Simplified Recovery System ---------- 17

4. Effects of Damping C_1 on ϕmax ---------- 38

5. Effects of Rod Length R_2 on ϕmax with C_1 Damping ---------- 39

6. Effects of RPV Mass on ϕmax with C_1 Damping --- 40

7. Effects of Horizontal Member Length R_1 on ϕmax with C_1 Damping ---------- 41

8. Effects of Moment of Inertia I_o on ϕmax with C_1 Damping ---------- 42

9. Linear Acceleration for Base Configuration ----- 46

10. Effects of Damping C_1 on ϕmax with C_2 Damping - 47

11. Effects of Damping C_2 on ϕmax ---------- 48

12. Effects of Rod Length R_2 on ϕmax with C_1, C_2 Damping ---------- 49

13. Effects of RPV Mass on ϕmax with C_1, C_2 Damping ---------- 50

14. Effects of Horizontal Member Length R_1 on ϕmax with C_1, C_2 Damping ---------- 51

15. Effects of Moment of Inertia I_o on ϕmax with C_1, C_2 Damping ---------- 52

16. Effects of Spring Constant K on ϕmax, with C_1, C_2 Damping ---------- 53

17. Pendulum Design A ---------- 55

18. Results of Pendulum A Analysis ---------- 57

19. Pendulum Design B ---------- 58

20. Results of Pendulum B Analysis ---------- 59

21. Computer Program ---------- 65

LIST OF SYMBOLS

D	- Rayleigh dissipation factor
ft	- Feet
g	- Acceleration of gravity, (32.2 ft/sec)
I_o	- Moment of Inertia of horizontal member about its pivot point, (ft-lb-sec^2)
K	- Spring constant of torsional spring located at pivot of horizontal member (ft-lb)
lb	- Pounds force
M	- Mass of RPV, (ft-lb-sec^2)
q	- Generalized coordinate
rad	- Radians, angular measure
R_1	- Length of horizontal member, (ft)
R_2	- Length of massless recovery rod corresponding to RPV distance from horizontal member following recovery (ft)
sec	- Second, unit of time
T	- Kinetic Energy, (ft-lbs)
V	- Potential Energy, (ft-lbs)
V_{RPV}	- Velocity expression for RPV (ft/sec)
x,y,z,	- Fixed axis coordinates
x',y',z'	- Moving axis coordinate
ζ	- Dimensionless damping ratio
θ, ϕ, ψ	- Coordinate system angles
ϕmax	- Maximum magnitude of angle ϕ

$\dot{\phi}_o$ - Initial condition on angular velocity

ω_n - Undamped natural frequency, (1/sec)

$\{\ \}$ - Column vector

$[\ ]$ - Matrix

$|\ |$ - Determinant

Note: Dot over a symbol represents differentiation with respect to time; i.e., $\dot{x}=dx/dt$

I. INTRODUCTION

Extensive efforts on Remotely Piloted Vehicles (RPV) have been underway for many years, covering a wide range of applications and missions, Ref. 1. It is only recently, however, that both the need and the technological capability for mini-RPVs have coalesced to the point that the development of these systems has become imperative. A mini-RPV is generally defined as an RPV that weighs less than 200 lbs mission loaded.

An essential part of an RPV system is the recovery system. The Army has recently experienced several mini-RPV losses due either directly or indirectly to the recovery method. The methods used to recover mini-RPV's vary from catching the RPV with an arresting cable similar in principle to that used on an aircraft carrier, to guiding the mini-RPV directly into a vertical net which is designed to flex and absorb the kinetic energy of the RPV. A completely satisfactory recovery system has not yet been established, hence studies into alternate recovery systems are of continuing interest to the Army.

The purpose of the analyses described herein was to model the dynamics of one alternate recovery system candidate, the "carousel" method. The carousel method was initially described as a candidate for a recovery procedure in a concept study performed by Teledyne Ryan for the Army,

Ref. 2, but the initial concept formulation did not include significant dynamic considerations. Therefore, the analyses conducted in this thesis, which are primarily oriented towards system dynamic response behavior, should serve in the role of providing additional information for concept feasibility considerations.

The carousel recovery system, shown in Figure 1, was conceptualized in this analysis as being composed of a vertical mast that supported a horizontal member which was allowed to rotate about the vertical mast. Hanging from the horizontal member are cables that will be caught by the wing tips of the approaching RPV. The RPV's kinetic energy will be dissipated by the recovery system through various means that will be evaluated in this analysis.

The RPV must be brought to rest without allowing excessive RPV swing since excessive swinging motion could result in the RPV hitting the recovery system structure. This consideration was of paramount concern when evaluating the merits of recovery system parameter variations.

For the purpose of this analysis the mini-RPV to be recovered was assumed to be the AQUILA, which is a U.S. Army mini-RPV developed by Lockheed Missiles and Space Company, Ref. 1, and is sketched in Figure 2. It has the following nominal characteristics: wing span, 12 ft; weight 150 lb; approach speed 50 knots; maximum loading, 6g vertical and axial, 3g lateral.

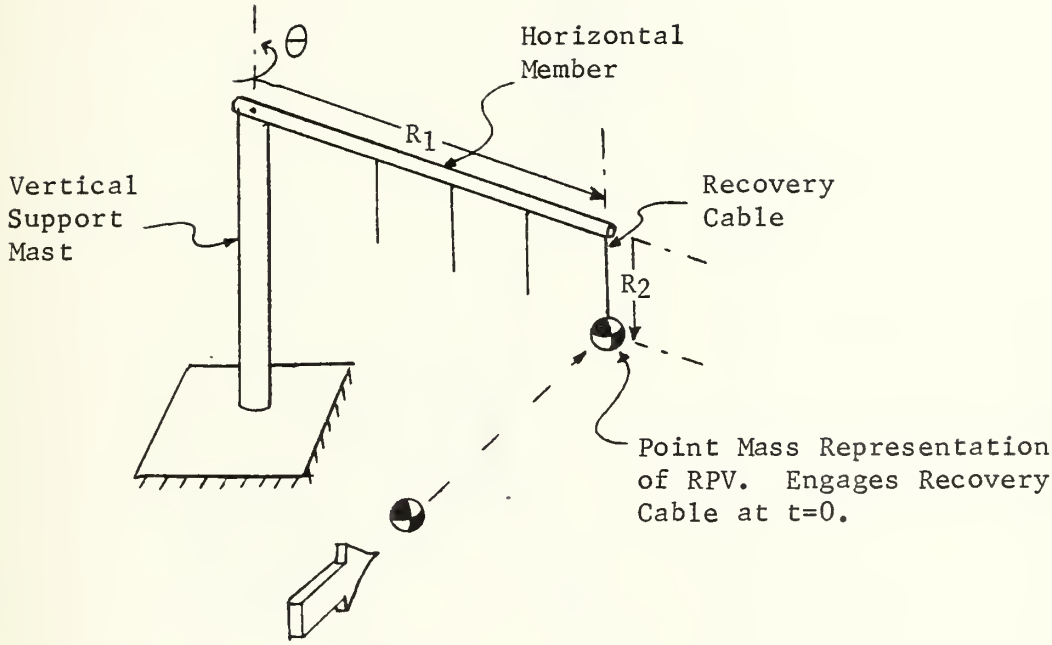

Figure 1 Carousel Recovery System

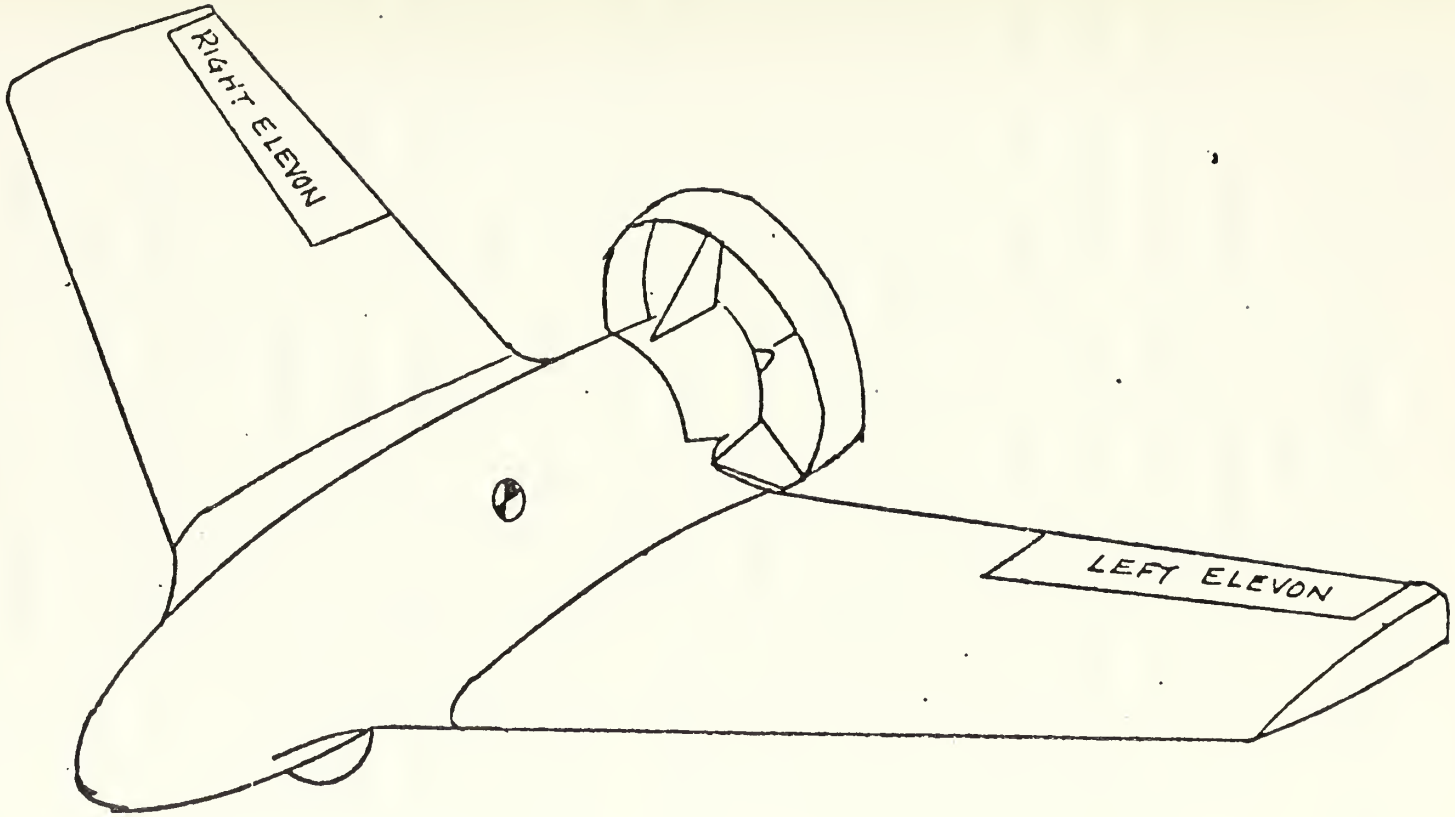

Figure 2 Aquila Mini-RPV

II. ANALYSIS

A. ASSUMPTIONS

Simplifying assumptions, as defined below, were made when establishing the equations of motion using the procedures suggested by Lagrange's equations, Ref. 3, in order to establish the basic principles of the carousel recovery system dynamics. Inclusion of system details such as recovery boom elasticity and RPV mass moments of inertia were considered as items which might tend to mask the basic question of feasibility at the present stage of analysis. Under these assumptions, the results supported the viability of the carousel recovery method and a basis was established upon which further analyses may be performed when the simplifying assumptions are removed.

The recovery system was initially assumed to be conservative, that is, friction losses were ignored and as soon as the RPV contacted the recovery system the engine was secured. This assumption was subsequently changed by the addition of damping to the recovery system configuration. The horizontal member was assumed to be rigid. A careful choice of material and structural characteristics for the horizontal member can minimize its dynamics and allow it to be approximated by a rigid member. The cables hanging from the horizontal member were replaced by massless thin recovery rods. The RPV was treated as a point mass and was

captured by one recovery rod. Treating the RPV as a point mass simplified the coordinate system used in the analysis by allowing the mass moment of inertia of the RPV about its principal axes to be neglected. The RPV was also assumed to approach perpendicular to the plane formed by the horizontal member and the vertical recovery rod that caught it. The approach velocity of the RPV was assumed to transfer undiminished to the recovery rod giving the rod an initial angular velocity only in the ϕ direction. Reference should be made to Figure 3 where the orientation of the generalized coordinates θ, ϕ and ψ is portrayed. These coordinates are a form of Euler angles, independent of each other, that together completely specify the position of the RPV relative to the fixed reference frame x-y-z. First θ defines the rotation of the moving coordinate system x'-y'-z' about the fixed axis z. It describes the rotation of the horizontal member in the x-y plane. Next ϕ defines the motion of the RPV about x' within the moving coordinate system. This is portrayed in Figure 3 as the motion of the RPV projected on the y'-z' plane. Finally, ψ depicts the remaining motion of the RPV after it rotates through θ and ϕ.

The system identified in Figure 3 is the reference or base configuration that was assumed for the analysis based on judgement of the RPV's weight and size. In this reference configuration the horizontal member, R_1, was 28 ft long and made of 6-inch aluminum I-beam having a mass moment of inertia of 1159 ft-lb-sec^2 about pivot "O".

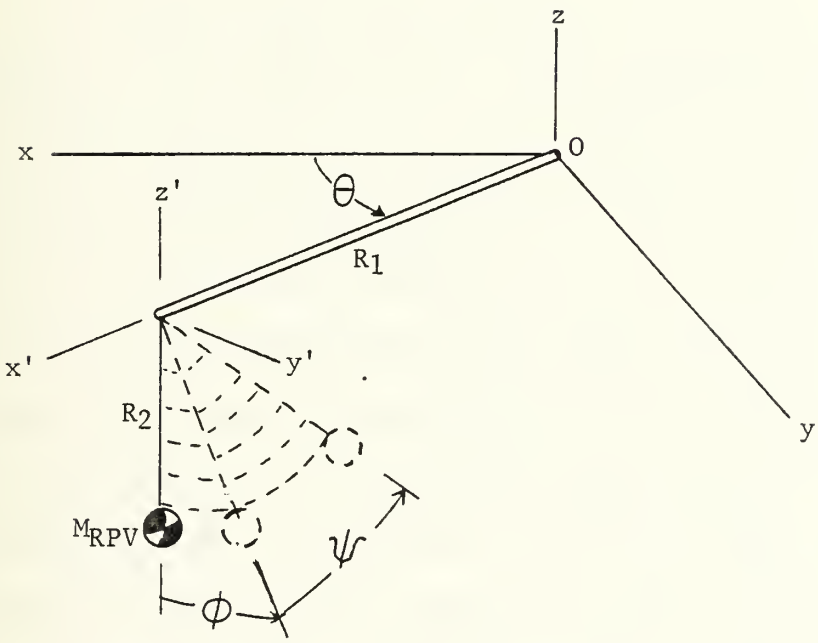

Figure 3 Simplified Recovery System

The recovery rod R_2, was 6 ft long. The RPV of mass 4.66 slugs (150 lbs) was suspended at the lower end of R_2. With an assumed approach speed of 50 knots (84.4 ft/sec), the initial angular velocity, $\dot{\phi}_o$, of the massless rod R_2 was 14 rad/sec according to the relation of equation (1):

$$\dot{\phi}_o = \frac{\text{Approach velocity (ft/sec)}}{R_2 \text{ (ft)}} \tag{1}$$

A linear, torsional spring, of spring constant K, located at "O", the pivot of the horizontal member, was initially used to resist the rotation of the horizontal member. Without any damping in this reference configuration it was further assumed that the spring's stored energy could be eliminated from the system through a ratchet release mechanism, after the horizontal member had swung through its initial maximum displacement. The ratchet mechanism was not modeled, as it was felt, and later confirmed by the results, that the critical motion of the RPV would occur shortly after impact with the recovery system. Simulation of the ratchet mechanism would have no effect on these results.

B. OVERVIEW OF ANALYSIS

The general approach of the analysis was to model the RPV motion after engagement with the recovery system using the generalized coordinate system $\theta-\phi-\psi$ indicated in Fig. 3. If the assumptions of a rigid horizontal member and a point mass RPV representation were removed, a minimum

of five more generalized coordinates would have been required. The equations of motion for the three degree of freedom system were obtained using Lagrange's equations for a conservative system. From these equations the acceleration, velocity and position of the RPV as a function of time were obtained in component form along each coordinate direction through the use of the Continuous System Modeling Program (CSMP). The input parameters were then varied and their effect on resulting dynamic motion studied.

Changes to the basic recovery system which included the addition of damping terms were later entertained as a consequence of initial results.

C. DETAILED ANALYSIS

1. Lagrange's Equation

The equations of motion were established using Lagrange's equation, Ref. 3. Three equations of motion were obtained for the system, since there were by assumption only three generalized coordinates: the coordinates θ, ϕ and ψ, as defined in Fig. 3. Lagrange's equation in the conservative form, without any generalized forces, is:

$$\frac{d}{dt}\left(\frac{\partial T}{\partial \dot{q}_i}\right) - \frac{\partial T}{\partial q_i} + \frac{\partial V}{\partial q_i} = 0; \qquad i = 1, 2, 3, \tag{2}$$

where

q_i = generalized coordinate ($q_1 = \theta, q_2 = \phi, q_3 = \psi$)

$\dot{q}_i$ = time derivative of q_i coordinate

$T = T(q_i, \dot{q}_i)$ = Kinetic energy (ft-lb)

$V = V(q_i)$ = Potential energy (ft-lb)

The kinetic energy was defined relative to the inertial reference frame by the following expression:

$$T = \tfrac{1}{2} I_o \dot{\theta}^2 + \tfrac{1}{2} M V_{RPV}^2 \tag{3}$$

where

I_o = Moment of Inertia of the horizontal member about pivot point "O" (ft-lb-sec^2)

M = Mass of RPV (slugs)

$\dot{\theta}$ = Angular velocity in θ coordinate direction (rad/sec)

V_{RPV} = Velocity expression for RPV derived in the next section (ft/sec)

The potential energy included the gravitational term acting upon the RPV mass and the stored energy in the torsional constraint spring. Equation 4 expresses the potential energy relative to the inertial frame of reference as follows:

$$V = MgR_2\left(1 - \cos\phi \cos\psi\right) + \tfrac{1}{2} K \theta^2 \tag{4}$$

where

R_2 = length of recovery rod corresponding to RPV distance from the horizontal member following recovery, (ft)

K = spring constant of spring at pivot of horizontal member (ft-lb)

Since its exactness is critical to the evaluation of Lagrange's equations of motion, the RPV velocity is treated separately in the ensuing section using the generalized coordinates.

2. Derivation of RPV Velocity

To derive an expression for the RPV's velocity after impact with the recovery system, the position of the RPV within the moving x'-y'-z' coordinate system as a function of the generalized coordinates θ, ψ was transformed to the fixed inertial reference system x-y-z. The time derivative of the RPV's position, expressed as a function of the three generalized coordinates θ, ϕ and ψ and referenced to the fixed inertial system, represented the absolute velocity of the RPV.

The RPV's position within the moving frame x'-y'-z' was expressed as follows:

$$x' = -R_2 \sin\psi \tag{5a}$$

$$y' = R_2 \sin\phi \cos\psi \tag{5b}$$

$$z' = -R_2 \cos\phi \cos\psi \tag{5c}$$

Transformation to the fixed inertial coordinate system may be stated as:

$$\begin{Bmatrix} x \\ y \end{Bmatrix} = \begin{bmatrix} \cos\theta & -\sin\theta \\ \sin\theta & \cos\theta \end{bmatrix} \begin{Bmatrix} -R_2 \sin\psi \\ R_2 \sin\phi \cos\psi \end{Bmatrix} + \begin{Bmatrix} R_1 \cos\theta \\ R_1 \sin\theta \end{Bmatrix} \tag{6a}$$

$$z = z' = -R_2 \cos\phi \cos\psi \tag{6b}$$

In an alternate form, the three components expressing the absolute position of the RPV mass following recovery engagement may be expressed as:

$$x = R_1\cos\theta - R_2\sin\psi\cos\theta - R_2\sin\phi\cos\psi\sin\theta \tag{7a}$$

$$y = R_1\cos\theta - R_2\sin\psi\sin\theta + R_2\sin\phi\cos\psi\cos\theta \tag{7b}$$

$$z = -R_2\cos\phi\cos\psi \tag{7c}$$

The absolute velocity of the RPV was obtained by taking the first time derivative of equation 7, thereby yielding:

$$\dot{x} = \left[-R_1\sin\theta + R_2(\sin\psi\sin\theta - \sin\phi\cos\psi\cos\theta)\right]\dot{\theta} - (R_2\cos\phi\cos\psi\sin\theta)\dot{\phi} + R_2(\sin\phi\sin\psi\sin\theta - \cos\psi\cos\theta)\dot{\psi} \tag{8a}$$

$$\dot{y} = \left[R_1\cos\theta - R_2(\sin\psi\cos\theta + \sin\phi\cos\psi\sin\theta)\right]\dot{\theta} + (R_1\cos\phi\cos\psi\cos\theta)\dot{\phi} - R_2\left(\cos\psi\sin\theta + \sin\phi\sin\psi\cos\theta\right)\dot{\psi} \tag{8b}$$

$$\dot{z} = R_2\left[(\sin\phi\cos\psi)\dot{\phi} + (\cos\phi\sin\psi)\dot{\psi}\right] \tag{8c}$$

The expression desired for use in Lagrange's equation, $V_{RPV}{}^2$, was obtained by squaring the components separately then adding them; i.e.,

$$V_{RPV}{}^2 = \dot{x}^2 + \dot{y}^2 + \dot{z}^2 \tag{9}$$

The expressions for $\dot{x}^2$, $\dot{y}^2$ and $\dot{z}^2$ are equations 10a, b and c.

$$\dot{x}^2 = \left[-R_1\sin\theta + R_2(\sin\psi\sin\theta - \sin\phi\cos\psi\cos\theta)\right]^2 \dot{\theta}^2$$

$$+R_2^2\cos^2\phi\cos^2\psi\sin^2\theta\,\dot{\phi}^2$$

$$+R_2^2(\sin\phi\sin\psi\sin\theta - \cos\psi\cos\theta)^2\dot{\psi}^2$$

$$-2R_2\cos\phi\cos\psi\sin\theta\left[-R_1\sin\theta + R_2(\sin\psi\sin\theta - \sin\phi\cos\psi\cos\theta)\right]\dot{\theta}\,\dot{\phi}$$

$$+2R_2(\sin\phi\sin\psi\sin\theta - \cos\psi\cos\theta)\left[-R_1\sin\theta + R_2(\sin\psi\sin\theta - \sin\phi\cos\psi\cos\theta)\right]\dot{\theta}\,\dot{\psi}$$

$$-2R_2^2\cos\phi\cos\psi\sin\theta(\sin\phi\sin\psi\sin\theta - \cos\psi\cos\theta)\dot{\phi}\dot{\psi} \tag{10a}$$

$$\dot{y}^2 = \left[R_1\cos\theta - R_2(\sin\psi\cos\theta + \sin\phi\cos\psi\sin\theta)\right]^2\dot{\theta}^2 + R_2^2\cos^2\phi\cos^2\psi\cos^2\theta\,\dot{\phi}^2$$

$$+R_2^2\left[\cos\psi\sin\theta + \sin\phi\sin\psi\cos\theta\right]^2\dot{\psi}^2$$

$$+2R_2\cos\phi\cos\psi\cos\theta\left[R_1\cos\theta - R_2(\sin\psi\cos\theta + \sin\phi\cos\psi\sin\theta)\right]\dot{\theta}\,\dot{\phi}$$

$$-2R_2\left[\cos\psi\sin\theta + \sin\phi\sin\psi\cos\theta\right]\left[R_1\cos\theta - R_2(\sin\psi\cos\theta + \sin\phi\cos\psi\sin\theta\right]\dot{\theta}\,\dot{\psi}$$

$$-2R_2^2\cos\phi\cos\psi\cos\theta\left[\cos\psi\sin\theta + \sin\phi\sin\psi\cos\theta\right]\dot{\psi}\,\dot{\phi} \tag{10b}$$

$$\dot{z}^2 = R_2^{\,2}\left[\sin^2\phi\cos^2\psi\,\dot{\phi}^2+\cos^2\phi\sin^2\psi\,\dot{\psi}^2+2\sin\phi\cos\phi\right.$$
$$\left.\sin\psi\cos\psi\,\dot{\phi}\,\dot{\psi}\right] \tag{10c}$$

When $\dot{x}^2$, $\dot{y}^2$, $\dot{z}^2$ were combined, several cancellations occurred and the final expression for $V_{RPV}^{\,2}$ simplified to:

$$V_{RPV}^{\,2} = \left[R_1^{\,2}+R_2^{\,2}\sin^2\psi+R_2^{\,2}\sin^2\phi\cos^2\psi-2R_1R_2\sin\psi\right]\dot{\theta}^2$$
$$+R_2^{\,2}\cos^2\psi\,\dot{\phi}^2+R_2^{\,2}\dot{\psi}^2+2R_2\cos\phi\cos\psi(R_1-R_2\sin\psi)\,\dot{\theta}\,\dot{\phi}$$
$$+(-2R_1R_2\sin\phi\sin\psi+2R_2^{\,2}\sin\phi)\,\dot{\theta}\,\dot{\psi} \tag{11}$$

3. <u>Derivation of Equations of Motion</u>

a. θ Equation of Motion

Now that an expression for $V_{RPV}^{\,2}$ has been obtained, Lagrange's equation can be evaluated according to section II.C.1. The equation was evaluated for each generalized coordinate θ, ϕ and ψ. The θ equation of motion was obtained by evaluating the Lagrange's equation using the θ generalized coordinate.

$$\frac{d}{dt}\left(\frac{\partial T}{\partial\dot{\theta}}\right) - \frac{\partial T}{\partial\theta} + \frac{\partial V}{\partial\theta} = 0 \tag{12}$$

Again:

Kinetic energy, $T=\frac{1}{2}I_o\,\dot{\theta}^2+\frac{1}{2}MV_{RPV}^{\,2}$ (13)

Potential energy, $V=MgR_2\left[1-\cos\phi\cos\psi\right]+\frac{1}{2}K\theta^2$ (14)

$$\frac{\partial T}{\partial\theta} = 0 \tag{15}$$

$$\frac{\partial V}{\partial \theta} = K\theta \tag{16}$$

$$\frac{d}{dt}\left(\frac{\partial T}{\partial \dot{\theta}}\right) = I_o\ddot{\theta} + M\left[(R_1{}^2 + R_2{}^2\sin^2\psi + R_2{}^2\sin^2\phi\cos^2\psi - 2R_1R_2\sin\psi)\ddot{\theta}\right.$$

$$+R_2\cos\phi\cos\psi(R_1 - R_2\sin\psi)\ddot{\phi} + (-R_1R_2\sin\phi\sin\psi +$$

$$R_2{}^2\sin\phi)\ddot{\psi}$$

$$+(2R_2{}^2\sin\psi\cos\psi\dot{\psi} + 2R_2{}^2\sin\phi\cos\phi\cos^2\psi\,\dot{\phi}$$

$$-2R_2{}^2\sin^2\phi\cos\psi\sin\psi\,\dot{\psi} - 2R_1R_2\cos\psi\,\dot{\psi})\,\dot{\theta}$$

$$-R_2\sin\phi\cos\psi(R_1 - R_2\sin\psi)\,\dot{\phi}^2 - R_2\sin\psi\cos\phi(R_1 - R_2$$

$$\sin\psi)\,\dot{\phi}\,\dot{\psi}$$

$$-R_2{}^2\cos\psi\cos\phi\cos\psi\,\dot{\psi}\dot{\phi} - R_1R_2\cos\phi\sin\psi\dot{\phi}\,\dot{\psi} - R_1R_2$$

$$\sin\phi\cos\psi\,\dot{\psi}^2$$

$$\left.+R_2{}^2\cos\phi\,\dot{\phi}\,\dot{\psi}\right] \tag{17}$$

Substituting equations 15, 16 and 17 into equation 12 and dividing through by $(MR_2{}^2)$ yields the following θequation of motion:

$$\frac{I_o}{MR_2^2}+\left(\frac{R_1}{R_2}-\sin\psi\right)^2+\cos^2\psi\sin^2\phi\,)\,\ddot{\theta}$$

$$+\sin\phi\left(1-\frac{R_1}{R_2}\sin\psi\right)\ddot{\psi}$$

$$+\cos\phi\left(\frac{R_1}{R_2}\cos\psi-\tfrac{1}{2}\sin 2\psi\right)\ddot{\phi}$$

$$+\sin 2\psi\cos^2\phi\ -2\frac{R_1}{R_2}\cos\psi)\,\dot{\psi}\,\dot{\theta}$$

$$+\sin 2\phi\cos^2\psi\ \dot{\phi}\,\dot{\theta}$$

$$+\cos\phi\left(-2\frac{R_1}{R_2}\sin\psi-\cos 2\psi+1\right)\dot{\phi}\,\dot{\psi}$$

$$-\sin\phi\left(\frac{R_1}{R_2}\cos\psi-\tfrac{1}{2}\sin 2\psi\right)\dot{\phi}^2$$

$$-\frac{R_1}{R_2}\sin\phi\cos\psi\,\dot{\psi}^2$$

$$+\frac{K\theta}{MR_2^2}=0 \tag{18}$$

b. ϕ Equation of Motion

Similarly the ϕ equation of motion was obtained from the following Lagrange's equation:

$$\frac{d}{dt}\left(\frac{\partial T}{\partial\dot{\phi}}\right)-\frac{\partial T}{\partial\phi}+\frac{\partial V}{\partial\phi}=0 \tag{19}$$

where

$$\frac{d}{dt}\left(\frac{\partial T}{\partial \dot{\phi}}\right) = M\Big[R_2{}^2\cos^2\psi\ddot{\phi} + R_2\cos\phi\cos\psi(R_1 - R_2\sin\psi)\ddot{\theta}$$

$$-2R_2{}^2\cos\psi\sin\psi\,\dot{\psi}\dot{\phi} - R_2\sin\phi\cos\psi(R_1 - R_2\sin\psi)\dot{\phi}\dot{\theta}$$

$$-R_2\sin\psi\cos\phi(R_1 - R_2\sin\psi)\dot{\theta}\dot{\psi} - R_2{}^2\cos\phi\cos^2\psi\,\dot{\psi}\dot{\theta}\Big] \tag{20}$$

$$\frac{\partial T}{\partial \phi} = M\Big[R_2{}^2\sin\phi\cos\phi\cos^2\psi\dot{\theta}^2 - R_2\sin\phi\cos\psi(R_1 - R_2\sin\psi)\dot{\theta}\dot{\phi}$$

$$+(-R_1R_2\cos\phi\sin\psi + R_2{}^2\cos\phi)\dot{\theta}\dot{\psi}\Big] \tag{21}$$

$$\frac{\partial V}{\partial \phi} = MgR_2\sin\phi\cos\psi \tag{22}$$

Substituting equations 20, 21 and 22 into equation 19 and dividing through by $(MR_2{}^2)$ yields the following ϕ equation of motion:

$$\left[\frac{R_1}{R_2}\cos\phi\cos\psi - \tfrac{1}{2}\cos\phi\sin 2\psi\right]\ddot{\theta}$$

$$+\cos^2\psi\,\ddot{\phi}$$

$$-\sin 2\psi\,\dot{\psi}\dot{\phi}$$

$$-\cos\phi(\cos 2\psi + 1)\dot{\theta}\dot{\psi}$$

$$-\tfrac{1}{2}\sin 2\phi\cos^2\psi\,\dot{\theta}^2$$

$$+\frac{g}{R_2}\sin\phi\cos\psi = 0 \tag{23}$$

c. ψ Equation of Motion

The ψ equation of motion was similarly obtained using the following Lagrange's equation:

$$\frac{d}{dt}\left(\frac{\partial T}{\partial \dot{\psi}}\right) - \frac{\partial T}{\partial \psi} + \frac{\partial V}{\partial \psi} = 0 \tag{24}$$

where

$$\frac{d}{dt}\left(\frac{\partial T}{\partial \dot{\psi}}\right) = R_2{}^2 M\left[\ddot{\psi} + \left(-\frac{R_1}{R_2}\cos\phi\sin\psi + \cos\phi\right)\dot{\phi}\dot{\theta} - \frac{R_1}{R_2}\cos\psi\sin\phi\,\dot{\psi}\dot{\theta}\right.$$
$$\left. + \left(-\frac{R_1}{R_2}\sin\phi\sin\psi + \sin\phi\right)\ddot{\theta}\right] \tag{25}$$

$$\frac{\partial T}{\partial \psi} = R_2{}^2 M\left[\left(\sin\psi\cos\psi - \sin^2\phi\,\cos\psi\sin\psi - \frac{R_1}{R_2}\cos\psi\right)\dot{\theta}^2\right.$$
$$-\cos\psi\sin\psi\,\dot{\phi}^2 + \left(-\frac{1}{R_2}\cos\phi\sin\psi(R_1 - R_2\sin\psi) - \cos^2\psi\right.$$
$$\left.\cos\phi\right)\dot{\theta}\dot{\phi}$$
$$\left. - \frac{R_1}{R_2}\sin\phi\cos\psi\,\dot{\theta}\dot{\psi}\right] \tag{26}$$

$$\frac{\partial V}{\partial \psi} = \frac{g}{R_2}\cos\phi\sin\psi \tag{27}$$

Substituting equations 25, 26 and 27 into equation 24 and dividing through by the $(MR_2{}^2)$ yields the following ψ equation of motion:

$$(-\frac{R_1}{R_2}\sin\phi\sin\psi+\sin\phi)\ddot{\theta}+\ddot{\psi}$$

$$+\cos\phi(1+\cos2\psi)\dot{\theta}\dot{\phi}$$

$$+(\tfrac{1}{2}\sin2\psi(\sin^2\phi-1)+\frac{R_1}{R_2}\cos\psi)\dot{\theta}^2$$

$$+\tfrac{1}{2}\sin2\psi\,\dot{\phi}^2+\frac{g}{R_2}\cos\phi\sin\psi=0 \qquad (28)$$

4. Solving the Equations of Motion

The equations of motion were solved for time history information of the RPV's position, velocity and acceleration using the IBM Continuous System Modeling Program (CSMP) which was available as resident software on the IBM 360-67 computer located in the W.R. Church Computer Center, Naval Postgraduate School. The use of CSMP as a high-level programming tool is quite similar to the familiar engineering language of FORTRAN, and programming details may be found in the test by Speckhart and Green, Ref. 5. Details of the actual program used are presented in the Appendix. To use this software package, the three equations of motion were first solved for the highest order derivative $\ddot{\theta}$, $\ddot{\phi}$ and $\ddot{\psi}$ in terms of the three generalized coordinates and their first time derivatives. Then, in a manner similar to an analog computer solution of differential equations, the CSMP program proceeded to integrate these equations numerically for values for $\dot{\theta}$, $\dot{\phi}$, $\dot{\psi}$, θ, ϕ and ψ, which were fed back into the equations for $\ddot{\theta}$, $\ddot{\phi}$ and $\ddot{\psi}$. This iterative method of

solution was repeated at each time increment. The resulting values for θ, ϕ and ψ were listed as a function of time and from these the motion the RPV was studied to assess the feasibility of the recovery system when a particular set of structural parameters and initial RPV conditions was specified.

Since the governing equations of motion (eqns. 18, 23 and 28) were inertially cross coupled, it was necessary to rearrange the equations into an inertially uncoupled form that would be acceptable for solution by the CSMP. In matrix form, equations 18, 23 and 28 may be expressed as;

$$\begin{bmatrix} a_{11} & a_{12} & a_{13} \\ a_{21} & 0 & a_{23} \\ a_{31} & a_{32} & 0 \end{bmatrix} \begin{Bmatrix} \ddot{\theta} \\ \ddot{\psi} \\ \ddot{\phi} \end{Bmatrix} = \begin{Bmatrix} b_1 \\ b_2 \\ b_3 \end{Bmatrix} \tag{29}$$

where

$$a_{11} = \frac{I_o}{M_2 R_2} + \left(\frac{R_1}{R_2} - \sin\psi\right)^2 + \cos^2\psi \sin^2\phi \tag{30a}$$

$$a_{12} = a_{31} = \sin\phi\left(1 - \frac{R_1}{R_2}\sin\psi\right) \tag{30b}$$

$$a_{13} = a_{21} = \cos\phi\left(\frac{R_1}{R_2}\cos\psi - \tfrac{1}{2}\sin^2\psi\right) \tag{30c}$$

$$a_{23} = \cos^2\psi \tag{30d}$$

$$a_{32} = 1 \tag{30e}$$

$$b_1 = \frac{R_1}{R_2}\sin\phi\cos\psi\,\dot{\psi}^2+\sin\phi\left(\frac{R_1}{R_2}\cos\psi-\tfrac{1}{2}\sin 2\psi\right)\dot{\phi}^2$$

$$-\left(\sin^2\psi\cos^2\phi-2\frac{R_1}{R_2}\cos\psi\right)\dot{\theta}\,\dot{\psi}-\sin 2\phi\cos^2\psi\,\dot{\theta}\,\dot{\phi}$$

$$-\left(1-\cos 2\psi-2\frac{R_1}{R_2}\sin\psi\right)\cos\phi\,\dot{\psi}\,\dot{\phi}-\frac{K}{M_2R_2^2}\theta \tag{30f}$$

$$b_2 = \tfrac{1}{2}\cos^2\psi\sin 2\phi\,\dot{\theta}^2+\cos\phi(1+\cos 2\psi)\dot{\theta}\,\dot{\phi}+\sin 2\psi\,\dot{\psi}\,\dot{\phi}-$$

$$\frac{g}{R_2}\sin\phi\cos\psi \tag{30g}$$

$$b_3 = \left(\tfrac{1}{2}\sin 2\psi\cos^2\phi-\frac{R_1}{R_2}\cos\psi\right)\theta^2-\tfrac{1}{2}\sin 2\psi\,\dot{\phi}^2-\cos\phi(1+$$

$$\cos 2\psi)\dot{\theta}\,\dot{\phi}-\frac{g}{R_2}\cos\phi\sin\psi \tag{30h}$$

Substituting equations 30a through 30h in matrix expression 29, $\ddot{\theta}$, $\ddot{\phi}$ and $\ddot{\psi}$ were solved using Cramers' rule, Ref. 4.

$$\ddot{\theta} = \frac{|A_1|}{|A|} \quad (31a) \qquad \ddot{\psi} = \frac{|A_2|}{|A|} \quad (31b) \qquad \ddot{\phi} = \frac{|A_3|}{|A|} \quad (31c)$$

where

$$|A| = \begin{vmatrix} a_{11} & a_{12} & a_{13} \\ a_{21} & 0 & a_{23} \\ a_{31} & a_{32} & 0 \end{vmatrix} = a_{12}\,a_{23}\,a_{31}-a_{11}\,a_{23}+a_{21}\,a_{13} \tag{32a}$$

$$|A_1| = \begin{vmatrix} b_1 & a_{12} & a_{13} \\ b_2 & 0 & a_{23} \\ b_3 & 1 & 0 \end{vmatrix} = b_3\,a_{12}\,a_{23}-b_1\,a_{23}+b_2\,a_{13} \tag{32b}$$

$$|A_2| = \begin{vmatrix} a_{11} & b_1 & a_{13} \\ a_{21} & b_2 & a_{23} \\ a_{31} & b_3 & 0 \end{vmatrix} = a_{31}(b_1a_{23}-b_2a_{13})-b_3(a_{11}a_{23}-a_{21}a_{13}) \tag{32c}$$

$$|A_3| = \begin{vmatrix} a_{11} & a_{12} & b_1 \\ a_{21} & 0 & b_2 \\ a_{31} & 1 & b_3 \end{vmatrix} = a_{31}(b_2a_{12})-(b_2a_{11}-b_1a_{21})+b_3(-a_{21}a_{12}) \tag{32d}$$

Equations 30a through 32d were programmed on the IBM 360-67 computer using CSMP, the details of which are described in the Appendix. The program evaluated $\ddot{\theta}$, $\ddot{\phi}$, $\ddot{\psi}$, $\dot{\theta}$, $\dot{\phi}$, $\dot{\psi}$, θ, ϕ and ψ as a function of time from the initial condition of RPV impact. The evaluation of the computer generated time history results is described in the next section.

III. SYSTEM DESIGN ANALYSIS AND RESULTS

A. UNDAMPED SYSTEM

The reference or base configuration of the recovery system described in section II.A. and Fig. 3 was the first configuration considered in the analysis. From this configuration each parameter was varied individually for various RPV approach speeds to assess the system's sensitivity to their changes.

From the outset of the investigation it was felt, as supported by early results, that the motion of the RPV along the ϕ coordinate would be a primary system constraint. A guideline value for ϕmaximum (ϕmax) was chosen to be 90 degrees, which corresponds to the recovery rod (R_2) reaching the horizontal. For the recovery system to pass its first requirement, an RPV approaching at 50 knots would have to be recovered with the maximum amplitude of ϕ not exceeding 90 degrees.

The results of modeling the reference configuration suggested that energy disipation would have to be included to bring ϕmax down to 90 degrees or less. Without any damping the system exhibited unacceptably high magnitudes for ϕ that corresponded to the RPV completely rotating about the horizontal member when approach speeds exceeded 25 knots. This can be seen by referring to Table I where ϕ is listed for the base configuration as a function of

TABLE I

VARIATION FOR UNDAMPED SYSTEM

$\dot{\phi}$ (rad/sec)	2.0000	5.0000	7.0000	10.000	12.000	14.000
TIME (sec)			ϕ (rad)			
0.0	0.0	0.0	0.0	0.0	0.0	0.0
0.10000	0.18935	0.44307	0.58979	0.78482	0.90272	1.0136
0.20000	0.32978	0.73558	0.96111	1.2652	1.4627	1.6765
0.30000	0.40796	0.92390	1.2180	1.6784	2.2017	3.5147
0.40000	0.42452	1.0343	1.4076	2.6862	4.0928	4.3561
0.50000	0.37936	1.0723	1.5703	4.2037	4.4554	4.6785
0.60000	0.28953	1.0222	2.0462	4.4841	4.7384	5.1160
0.70000	9.64689E-02	0.80713	4.5237	4.7156	5.1223	5.6269
0.80000	-0.10772	0.12095	4.6735	5.0143	5.5901	6.2410
0.90000	-0.28043	-0.68628	4.8115	5.4054	6.1806	6.9074
1.0000	-0.39014	-0.95149	4.9835	5.9136	6.8328	10.201
1.1000	-0.43512	-1.0120	5.2192	6.6150	7.0489	9.7818
1.2000	-0.41761	-0.97423	5.5496	7.0821	8.9427	9.1263
1.3000	-0.33679	-0.85848	6.0551	7.3121	8.5277	8.5524
1.4000	-0.19074	-0.65810	6.7084	4.1726	2.9531	8.0154
1.5000	7.09220E-03	-0.34186	7.1385	3.9618	2.4365	7.4746
1.6000	0.20331	0.11540	7.4273	3.7130	1.9794	6.2464
1.7000	0.34667	0.51472	7.6443	3.4176	1.5338	4.9576
1.8000	0.42577	0.77584	7.8505	3.0834	0.89049	4.3154
1.9000	0.44307	0.94231	9.2141	2.7559	-0.80793	3.5926
2.0000	0.39968	1.0336	10.749	2.4721	-1.3203	2.5848
2.1000	0.29372	1.0515	10.882	2.2297	-1.6348	1.8557
2.2000	0.12613	0.97429	11.002	1.9808	-1.9378	-0.12271
2.3000	-7.59115E-02	0.70481	11.159	-0.92594	-2.1755	-0.82250
2.4000	-0.25224	-0.22832E-02	11.370	-0.61076	-2.3034	-0.49276
2.5000	-0.36754	-0.74426	11.660	-1.56873E-02	-2.4049	0.36464
2.6000	-0.41868	-0.96575	12.077	0.61346	-2.9720	0.97366
2.7000	-0.40820	-1.0176	12.733	1.0625	-4.8372	1.2088
2.8000	-0.35604	-0.97792	13.282	1.4238	-5.8238	-1.3808
2.9000	-0.20081	-0.85209	13.634	1.6964	-6.6196	-1.8534
3.0000	-1.31300E-02	-0.66231	13.896	1.9193	-6.7906	-2.1491
3.1000	0.18036	-0.34717	14.126	2.2504	-6.7060	-2.5662
3.2000	0.32759	0.11093	14.489	3.8380	-6.4944	-3.0024
3.3000	0.41271	0.51450	16.533	4.6618	-6.3032	-3.2816
3.4000	0.43621	0.77915	17.022	5.1189	-6.2370	-3.3063
3.5000	0.39634	0.94900	17.198	5.6832	-6.3371	-2.6350
3.6000	0.29640	1.0444	17.370	6.6104	-6.5617	-0.22018
3.7000	0.13020	1.0683	17.582	7.2808	-6.5706	0.35697
3.8000	-7.36532E-02	1.0032	17.864	7.7414	-3.6508	0.29071
3.9000	-0.23259	0.77118	18.263	8.1452	-3.3743	0.20596
4.0000	-0.36883	9.88471E-02	18.909	8.6944	-3.2090	0.32711
4.1000	-0.41815	-0.85400	19.517	9.9642	-3.1833	0.68832
4.2000	-0.40391	-0.91351	19.901	10.637	-3.2764	0.93689
4.3000	-0.32589	-0.97625	20.181	11.061	-3.4756	0.95298
4.4000	-0.18310	-0.93953	20.404	11.518	-3.7188	0.51699
4.5000	1.04145E-02	-0.82249	20.608	12.174	-3.9211	-1.3568
4.6000	0.20294	-0.61661	20.894	13.145	-4.0187	-2.1400
4.7000	0.34515	-0.28689	22.152	13.745	-2.5786	-3.0707
4.8000	0.42538	0.17538	23.248	14.209	-1.0654	-4.0335
4.9000	0.44556	0.55752	23.561	14.744	-0.41306	-4.7076
5.0000	0.40669	0.81022	23.815	15.947	0.49490	-5.4942
5.1000	0.30698	0.97386	24.109	16.730	1.0836	-6.9926
5.2000	0.14642	1.0665	24.511	17.099	1.5694	-7.7131

time after impact for approach speeds ranging from 7 knots ($\dot{\phi}_o$=2 rad/sec Ref. Equation 1) to 50 knots ($\dot{\phi}_o$=14 rad/sec). Note that for $\dot{\phi}_o$=7 rad/sec, or approximately a 25-knot approach speed, the magnitude of ϕ at 0.7 seconds after impact was greater than 180 degrees. The RPV has started to rotate over the horizontal member. Variation of the system parameters did not correct this deficiency.

B. DAMPING ADDED TO THE HORIZONTAL MEMBER

In an effort to correct the excessive RPV swing in the ϕ coordinate direction, a Rayleigh dissipative energy term, D, was introduced into Lagrange's equation:

$$\frac{d}{dt}\left(\frac{\partial T}{\partial \dot{q}_i}\right) - \frac{\partial T}{\partial q_i} + \frac{\partial V}{\partial q_i} + \frac{\partial D}{\partial \dot{q}_i} = 0 \tag{33}$$

where $D=\frac{1}{2}C_1\dot{\theta}^2$

This additional term precipitated through the equation of motion derivation of section II.C. with the addition of only a $C_1\dot{\theta}$ term to the θ equation of motion, equation 18. This change was easily incorporated into the computer program as indicated in the Appendix.

An initial estimate of the magnitude of the damping constant C_1 was obtained using the simplified linearized pendulum equation below. The damping value was varied to detect the system's sensitivity to C_1.

$$\ddot{\theta} + 2\zeta\omega_n\dot{\theta} + \omega_n^2\theta = 0 \tag{34}$$

where

$$\omega_n^2 = \frac{K}{I_o}$$

$$2\zeta\omega_n = \frac{C_1}{I_o}$$

For values of I_o=1159 lb-ft-sec^2, K=50 ft-lb and ζ= 0.15, which was selected to introduce just a small amount of damping, the initial estimate of C_1 was 75 ft-lb-sec.

The results of adding damping C_1 to the pivot of the horizontal member in the base configuration indicated that it was only partially successful in reducing ϕmax. This can be seen by referring to Table II where ϕ is listed for this configuration as a function of time after impact for approach speeds ranging from 7 knots, where $\dot{\phi}_o$=2 rad/sec, to 50 knots, where $\dot{\phi}_o$=14 rad/sec. Note that the magnitude of ϕ was still approaching 180 degrees for approach speed initial conditions in excess of 35 knots ($\dot{\phi}_o$=10 rad/sec).

Variation of system parameters including C_1 did little to further reduce ϕmax, as shown in Figures 4 through 8, where the base configuration of R_1=28 ft, R_2=6 ft, M=4.66 slugs, I_o=1159 ft-lbs-sec^2, K=50 ft-lb and C_1=75 ft-lb-sec is plotted with only the indicated parameter varied, ceteris paribus.

C. DAMPING ADDED TO RECOVERY ROD

In a further effort to reduce the maximum swing, ϕmax, of the recovery system, damping was also added to the

TABLE II

VARIATION WITH C_1 DAMPING

$\dot{\phi}$(rad/sec)	2.0000	5.0000	7.0000	10.000	12.000	14.000
TIME (sec)			ϕ (rad)			
0.0	0.0	0.0	0.0	0.0	0.0	0.0
0.10000	0.19123	0.45258	0.60659	0.81340	0.93909	1.0576
0.20000	0.34659	0.79420	1.0468	1.3891	1.6092	1.8392
0.30000	0.46649	1.0855	1.4095	1.9214	2.3298	2.8505
0.40000	0.55359	1.2853	1.7273	2.4860	3.0472	3.5996
0.50000	0.60549	1.4585	2.0044	2.8905	3.2009	3.3275
0.60000	0.62481	1.5835	2.2154	2.9641	3.1018	3.1367
0.70000	0.61186	1.6553	2.3257	2.8784	2.9255	2.8674
0.80000	0.56731	1.6691	2.3299	2.7326	2.7191	2.6178
0.90000	0.49298	1.6232	2.2496	2.5546	2.4928	2.3276
1.0000	0.39337	1.5183	2.1071	2.3509	2.2434	2.0043
1.1000	0.27745	1.3552	1.9146	2.1210	1.9628	1.6319
1.2000	0.15890	1.1316	1.6752	1.8605	1.6389	1.1954
1.3000	5.12783E-02	0.84070	1.3848	1.5607	1.2556	0.67426
1.4000	-3.80701E-02	0.47714	1.0302	1.2065	0.78794	7.60108E-02
1.5000	-0.10754	9.08231E-02	0.58566	0.76947	0.21264	-0.32779
1.6000	-0.15914	-0.18040	9.40856E-02	0.21986	-0.25774	-0.54042
1.7000	-0.19336	-0.34152	-0.23864	-0.24172	-0.51321	-0.66867
1.8000	-0.21133	-0.44852	-0.41787	-0.50010	-0.67199	-0.74375
1.9000	-0.21592	-0.52513	-0.53648	-0.66956	-0.77298	-0.77499
2.0000	-0.20725	-0.57883	-0.62734	-0.78632	-0.82778	-0.76385
2.1000	-0.18765	-0.60945	-0.69982	-0.85930	-0.83955	-0.70690
2.2000	-0.16019	-0.61292	-0.75129	-0.89042	-0.80784	-0.61051
2.3000	-0.12705	-0.58462	-0.77114	-0.87970	-0.73112	-0.47544
2.4000	-9.13231E-02	-0.52295	-0.74679	-0.82681	-0.60968	-0.32471
2.5000	-5.56887E-02	-0.43178	-0.67230	-0.73149	-0.45164	-0.17897
2.6000	-2.24051E-02	-0.32056	-0.55419	-0.59437	-0.27639	-5.83703E-02
2.7000	6.83791E-03	-0.20222	-0.40966	-0.41988	-0.11361	2.92516E-02
2.8000	3.09306E-02	-9.03940E-02	-0.25916	-0.22465	1.48990E-02	8.63093E-02
2.9000	4.92885E-02	4.09682E-03	-0.12053	-4.21316E-02	0.10572	0.12001
3.0000	6.17713E-02	7.61038E-02	-6.72598E-03	0.10271	0.16560	0.13804
3.1000	6.86021E-02	0.12595	7.65305E-02	0.20547	0.20339	0.14665
3.2000	7.02919E-02	0.15689	0.13100	0.28469	0.22225	0.14996
3.3000	6.75682E-02	0.17313	0.16255	0.33280	0.22944	0.14994
3.4000	6.15045E-02	0.17860	0.17828	0.35636	0.22659	0.14636
3.5000	5.24492E-02	0.17608	0.18499	0.35728	0.21494	0.13766
3.6000	4.19584E-02	0.16672	0.18729	0.33770	0.19498	0.12219
3.7000	3.07320E-02	0.15058	0.18584	0.30057	0.16725	0.10016
3.8000	1.95842E-02	0.12799	0.17764	0.25005	0.13316	7.39846E-02
3.9000	9.10750E-03	0.10063	0.15935	0.19138	9.53227E-02	4.71241E-02
4.0000	-1.45184E-04	7.14120E-02	0.13131	0.13026	5.70949E-02	2.25714E-02
4.1000	-7.86290E-03	4.35646E-02	9.79567E-02	7.17672E-02	2.17651E-02	2.20006E-03
4.2000	-1.38655E-02	1.93211E-02	6.46446E-02	1.95136E-02	-8.14128E-03	-1.31125E-02
4.3000	-1.81027E-02	8.90084E-05	3.53900E-02	-2.44869E-02	-3.11643E-02	-2.52693E-02
4.4000	-2.08313E-02	-1.41242E-02	1.21524E-02	-5.94488E-02	-4.69904E-02	-2.88113E-02
4.5000	-2.15690E-02	-2.40752E-02	-4.77048E-03	-8.53102E-02	-5.58237E-02	-3.06742E-02
4.6000	-2.11722E-02	-3.08753E-02	-1.63095E-02	-0.10241	-5.90127E-02	-3.00656E-02
4.7000	-1.98166E-02	-3.55572E-02	-2.40510E-02	-0.11133	-5.78143E-02	-2.80198E-02
4.8000	-1.71812E-02	-3.87649E-02	-2.96436E-02	-0.11281	-5.35084E-02	-2.51634E-02
4.9000	-1.41339E-02	-4.07278E-02	-3.43606E-02	-0.10777	-4.70877E-02	-2.17045E-02
5.0000	-1.07584E-02	-4.11119E-02	-3.88374E-02	-9.73029E-02	-3.92430E-02	-1.76649E-02
5.1000	-7.24189E-03	-3.94761E-02	-4.28766E-02	-8.26985E-02	-3.05178E-02	-1.31679E-02
5.2000	-3.86396E-03	-3.55748E-02	-4.53964E-02	-6.53483E-02	-2.14653E-02	-8.66103E-03

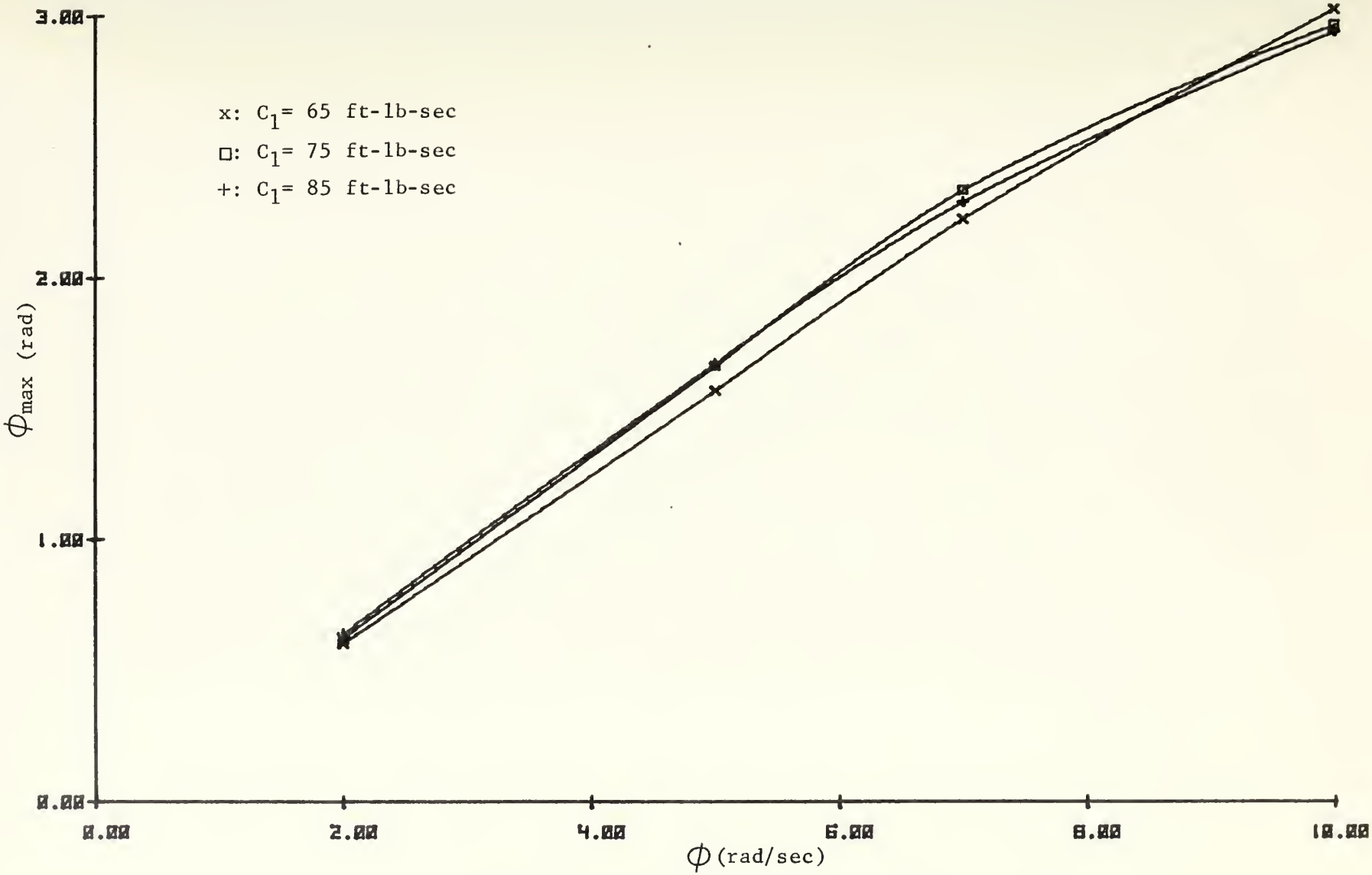

Figure 4 Effects of Damping C_1 on ϕ_{max}

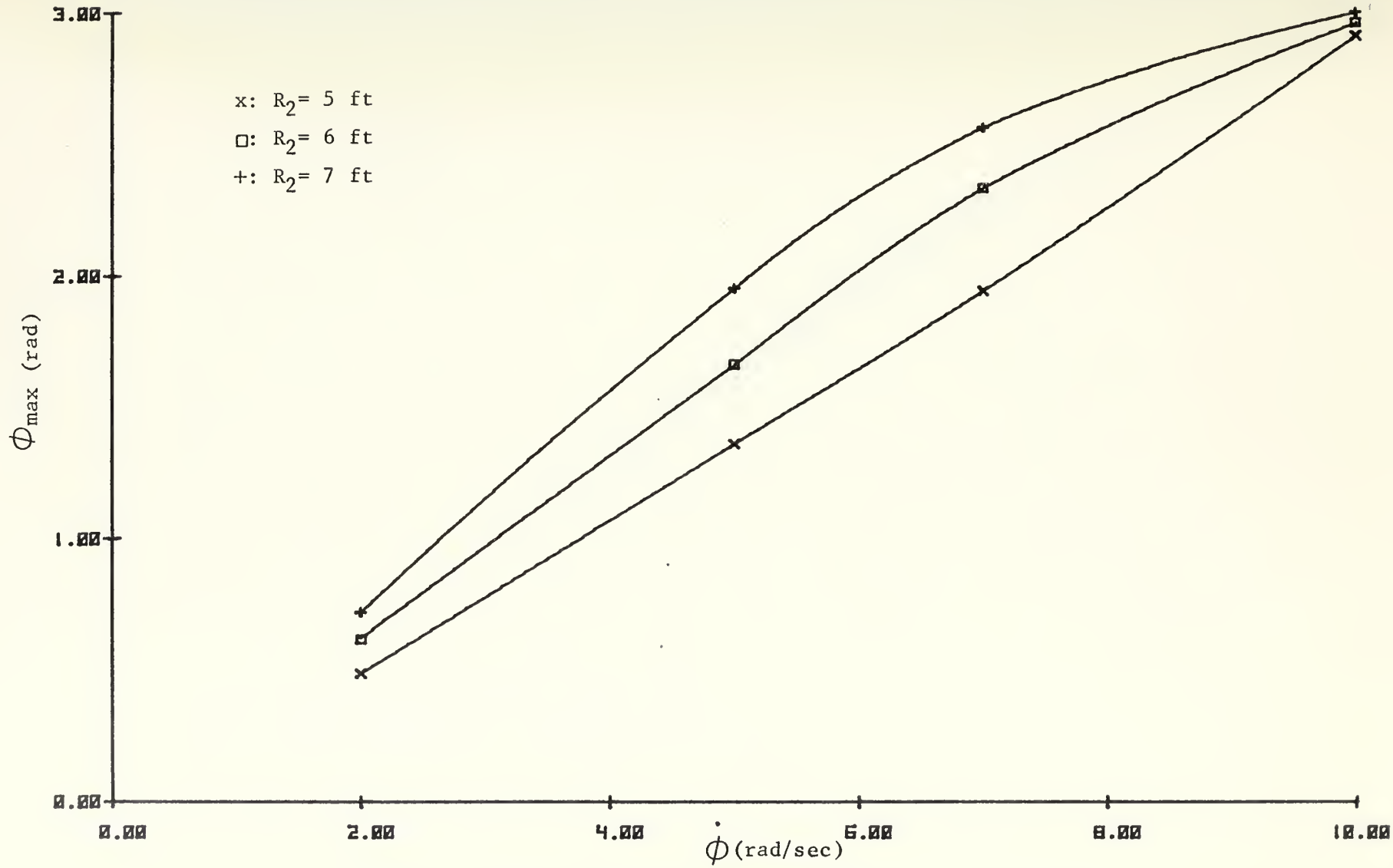

Figure 5 Effects of Rod Length R_2 on ϕ_{max} with C_1 Damping

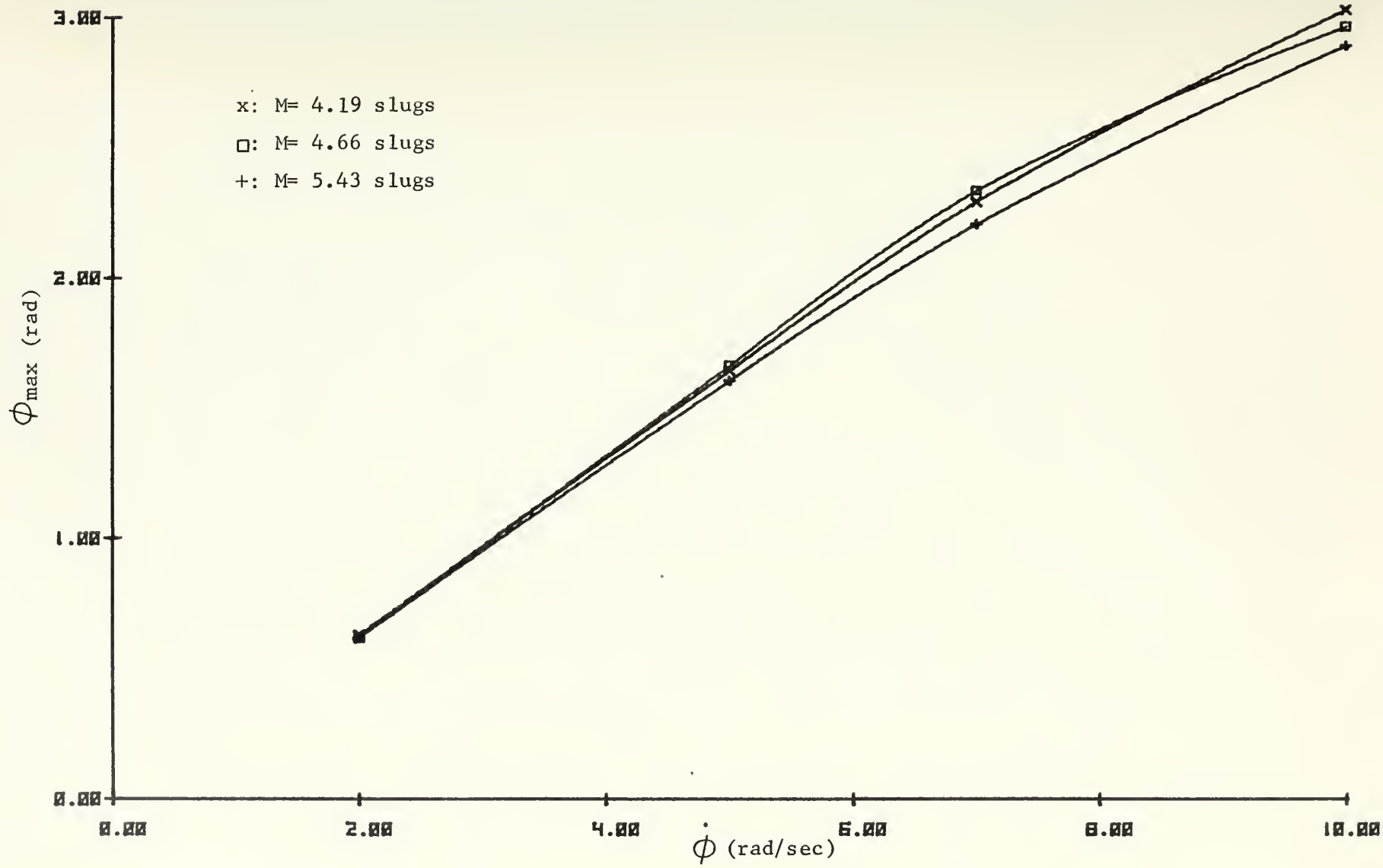

Figure 6 Effects of RPV Mass on ϕ_{max} with C_1 Damping

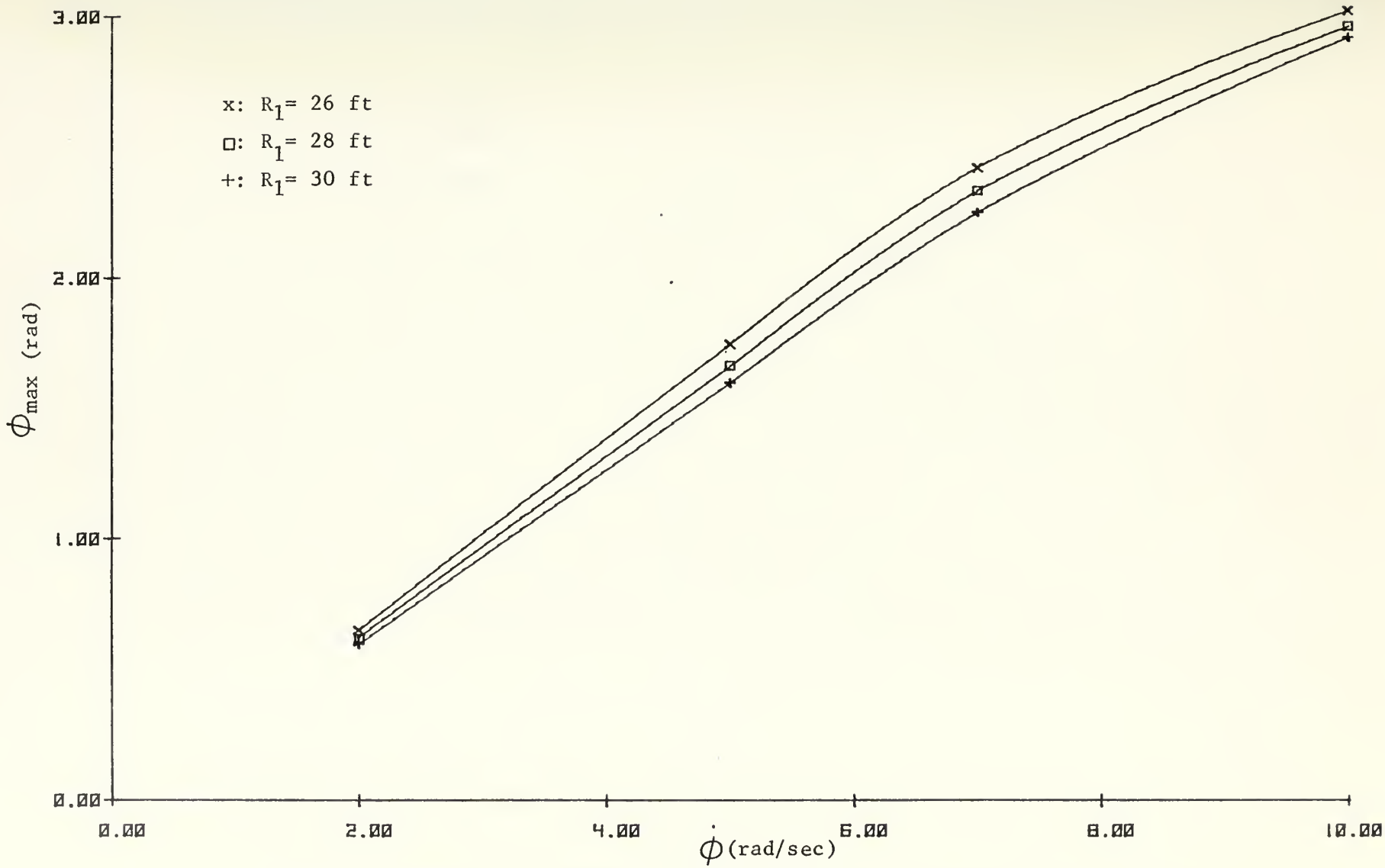

Figure 7 Effects of Horizontal Member Length R_1 on ϕ_{max} with C_1 Damping

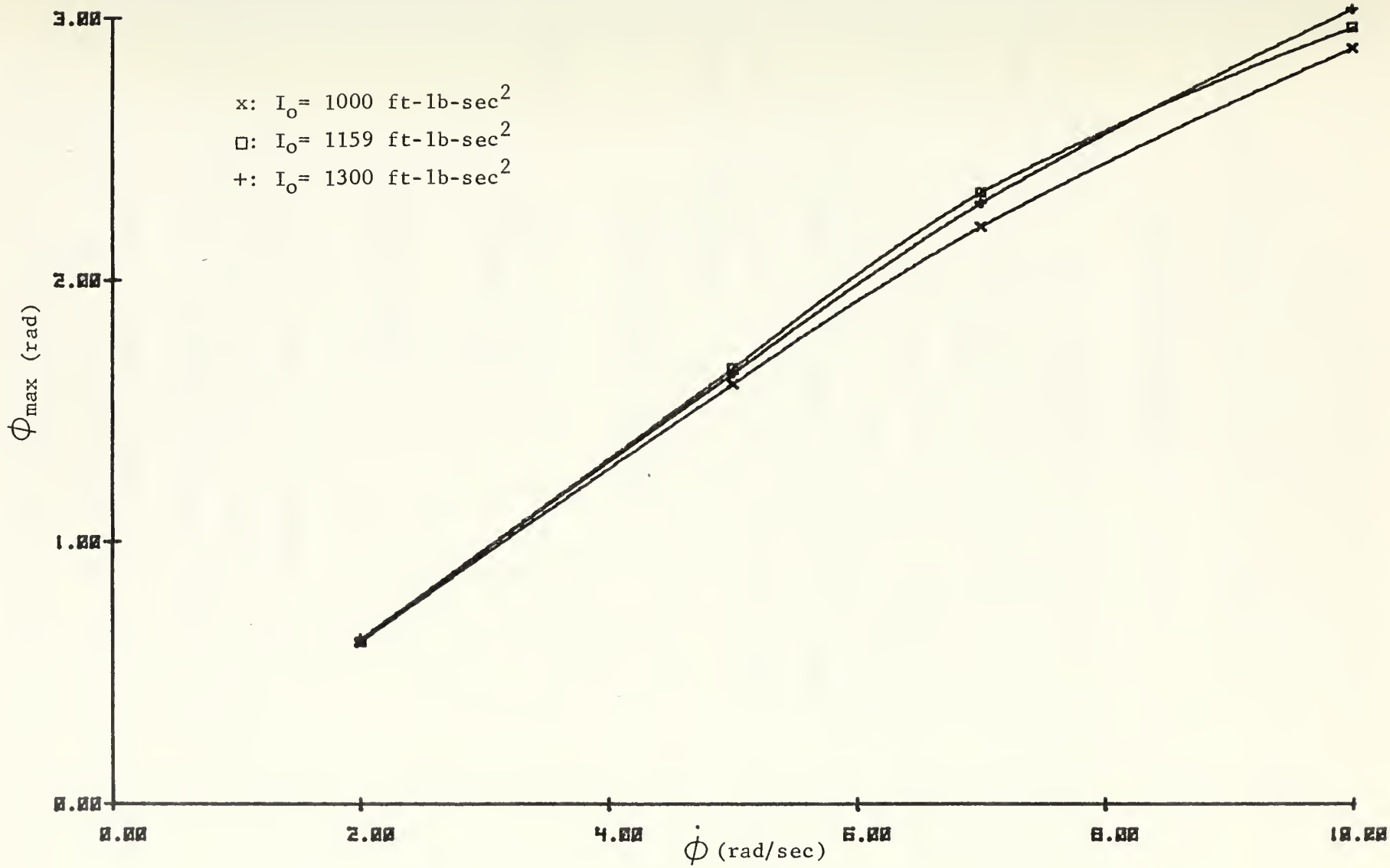

Figure 8 Effects of Moment of Inertia I_o on ϕ_{max} with C_1 Damping

recovery rod. The added damping was included in the system's model, without cross coupling, by modifying the Rayleigh dissipative energy function to the form of:

$$D=\tfrac{1}{2}C_1\dot{\theta}^2+\tfrac{1}{2}C_2\dot{\phi}^2 \tag{35}$$

The additional dissipation term precipitated through the equation of motion derivation described in section II.C. as the addition of a $C_2\dot{\phi}$ term to the ϕ equation of motion, equation 23. This change was also easily incorporated into the computer program as indicated in the Appendix.

An estimate of C_2 was obtained in a manner similar to that described in the previous section using the simple pendulum equation:

$$\ddot{\phi}+2\zeta\omega_n\dot{\phi}+\omega_n^2\phi=0 \tag{36}$$

where

$$2\zeta\omega_n=\frac{C_2}{MR_2^2}$$

$$\omega_n=\sqrt{\frac{g}{R_2}}$$

Only a slight amount of damping, C_2=3.24 ft-lb-sec, added to the recovery rod of the base configuration, in addition to the horizontal member damping, was sufficient to reduce ϕmax to approximately 90 degrees at RPV approach speeds of 50 knots ($\dot{\phi}_0$=14 rad/sec). This can be seen by referring to Table III where ϕ is listed as a function of

TABLE III

VARIATION WITH C_1, C_2 DAMPING

$\dot{\phi}$,(rad/sec)	2.0000	5.0000	7.0000	10.000	12.000	14.000
TIME (sec)			ϕ (rad)			
0.0	0.0	0.0	0.0	0.0	0.0	0.0
0.10000	0.12170	0.30011	0.41432	0.57716	0.68004	0.77870
0.20000	0.18238	0.44932	0.61917	0.85802	1.0085	1.1549
0.30000	0.22271	0.54671	0.75046	1.0370	1.2250	1.4206
0.40000	0.24809	0.60819	0.83306	1.1515	1.3703	1.6199
0.50000	0.26158	0.64202	0.87852	1.2159	1.4474	1.6491
0.60000	0.26662	0.65378	0.89478	1.2365	1.4756	1.5876
0.70000	0.26592	0.64812	0.88858	1.2225	1.4030	1.5231
0.80000	0.25558	0.62903	0.86475	1.1857	1.3464	1.4557
0.90000	0.24304	0.59931	0.82822	1.1340	1.2806	1.3814
1.0000	0.22755	0.56313	0.78155	1.0709	1.2057	1.2979
1.1000	0.21013	0.52112	0.72620	0.99780	1.1212	1.2037
1.2000	0.19162	0.47560	0.66558	0.91557	1.0268	1.0979
1.3000	0.17271	0.42819	0.59964	0.82521	0.93292	0.98117
1.4000	0.15394	0.38046	0.53117	0.72872	0.81174	0.85771
1.5000	0.13571	0.33364	0.46294	0.63019	0.69927	0.73635
1.6000	0.11833	0.28961	0.39804	0.53635	0.59607	0.63815
1.7000	0.10203	0.24864	0.33912	0.45473	0.51224	0.56374
1.8000	8.69552E-02	0.21145	0.28761	0.38910	0.44905	0.50621
1.9000	7.51801E-02	0.17816	0.24349	0.33764	0.40026	0.46182
2.0000	6.07480E-02	0.14865	0.20584	0.29602	0.35916	0.41996
2.1000	4.96530E-02	0.12264	0.17349	0.26058	0.32193	0.37717
2.2000	3.98605E-02	9.98640E-02	0.14543	0.22899	0.28665	0.33527
2.3000	3.16155E-02	8.00397E-02	0.12084	0.19988	0.25233	0.29324
2.4000	2.39381E-02	6.28626E-02	9.91612E-02	0.17250	0.21857	0.25104
2.5000	1.76491E-02	4.81240E-02	8.00338E-02	0.14649	0.18550	0.20981
2.6000	1.23543E-02	3.56195E-02	6.32377E-02	0.12191	0.15579	0.17130
2.7000	7.95760E-03	2.51575E-02	4.86633E-02	9.91184E-02	0.12455	0.13742
2.8000	4.36243E-03	1.65462E-02	3.62505E-02	7.87107E-02	9.89649E-02	0.10951
2.9000	1.47594E-03	9.58581E-03	2.59261E-02	6.12385E-02	7.78415E-02	8.76719E-02
3.0000	-7.98917E-04	4.06615E-03	1.75533E-02	4.69718E-02	6.12504E-02	7.10214E-02
3.1000	-2.54133E-03	-2.20450E-04	1.09157E-02	3.57652E-02	4.65088E-02	5.82451E-02
3.2000	-3.63396E-03	-3.47705E-03	5.73914E-03	2.71366E-02	3.67559E-02	4.81141E-02
3.3000	-4.74727E-03	-5.93394E-03	1.73840E-03	2.04802E-02	3.10769E-02	3.97022E-02
3.4000	-5.34621E-03	-7.69271E-03	-1.34041E-03	1.52374E-02	2.47916E-02	3.23659E-02
3.5000	-5.68770E-03	-8.90190E-03	-3.69757E-03	1.09840E-02	1.94264E-02	2.57731E-02
3.6000	-5.82175E-03	-9.66210E-03	-5.47837E-03	7.46114E-03	1.46942E-02	1.96721E-02
3.7000	-5.79136E-03	-1.00528E-02	-6.78228E-03	4.39971E-03	1.04238E-02	1.40524E-02
3.8000	-5.65573E-03	-1.01395E-02	-7.68205E-03	1.79555E-03	6.59552E-03	8.90176E-03
3.9000	-5.33053E-03	-9.97915E-03	-8.22849E-03	-4.19802E-04	3.19316E-03	4.37355E-03
4.0000	-5.05859E-03	-9.62465E-03	-8.47209E-03	-2.25778E-03	2.62264E-04	5.11748E-04
4.1000	-4.69040E-03	-9.12607E-03	-8.47062E-03	-3.73114E-03	-2.18199E-03	-2.68365E-03
4.2000	-4.29460E-03	-8.53003E-03	-8.23318E-03	-4.67292E-03	-4.16638E-03	-5.27155E-03
4.3000	-3.88640E-03	-7.87755E-03	-7.97267E-03	-5.35789E-03	-5.75093E-03	-7.22598E-03
4.4000	-3.47799E-03	-7.20195E-03	-7.59286E-03	-5.88762E-03	-6.99966E-03	-8.91661E-03
4.5000	-3.07839E-03	-6.52766E-03	-7.18179E-03	-6.87011E-03	-7.95371E-03	-1.00586E-02
4.6000	-2.69630E-03	-5.87058E-03	-6.75954E-03	-7.20765E-03	-8.62591E-03	-1.07736E-02
4.7000	-2.33545E-03	-5.23967E-03	-6.33135E-03	-7.40016E-03	-9.01801E-03	-1.10921E-02
4.8000	-1.99991E-03	-4.63918E-03	-5.89402E-03	-7.44009E-03	-9.14055E-03	-1.10586E-02
4.9000	-1.69187E-03	-4.07073E-03	-5.44211E-03	-7.32590E-03	-9.01596E-03	-1.07190E-02
5.0000	-1.41241E-03	-3.53496E-03	-4.97194E-03	-7.06513E-03	-8.67252E-03	-1.01155E-02
5.1000	-1.16170E-03	-3.03249E-03	-4.48317E-03	-6.67048E-03	-8.15647E-03	-9.28114E-03
5.2000	-9.39217E-04	-2.56441E-03	-3.97910E-03	-6.15689E-03	-7.43492E-03	-8.26965E-03

time after impact for approach speeds ranging from 7 knots ($\dot{\phi}_o$=2 rad/sec) to 50 knots ($\dot{\phi}_o$=14 rad/sec). The maximum magnitude of θ and ψ for the modified configuration at the 50-knot RPV approach speed was 50 degrees and 63 degrees, respectively.

Further study of the modified base configuration was performed to obtain the magnitude of the RPV's linear acceleration. The absolute value of the RPV's linear acceleration was obtained using the following equation:

$$\text{Acceleration} = \sqrt{\ddot{x}^2+\ddot{y}^2+\ddot{z}^2} \tag{37}$$

where x, y and z are defined by equations 7a, b and c. A plot of equation 37 as a function of time for the modified base configuration is presented in Figure 9. It may be noted that the magnitude reduces to below one "g" within one second after the RPV contacts the recovery system.

The sensitivity of ϕmax to each of the system parameters is indicated in Figures 10 through 16, where the base configuration of R_1=28 ft, R_2=6 ft, M=4.66 slugs, I_o=1159 ft-lb=sec^2, K=50 ft-lb, C_1=75 ft-lb-sec and C_2= 3.24 ft-lb-sec is plotted with only the indicated parameter varied, ceteris paribus. It can be noted from Figure 12 that the system was sensitive to the recovery rod length, R_2, which may be interpreted as an implication that the engagement point for RPV capture on the vertical cables has considerable importance to system dynamic response.

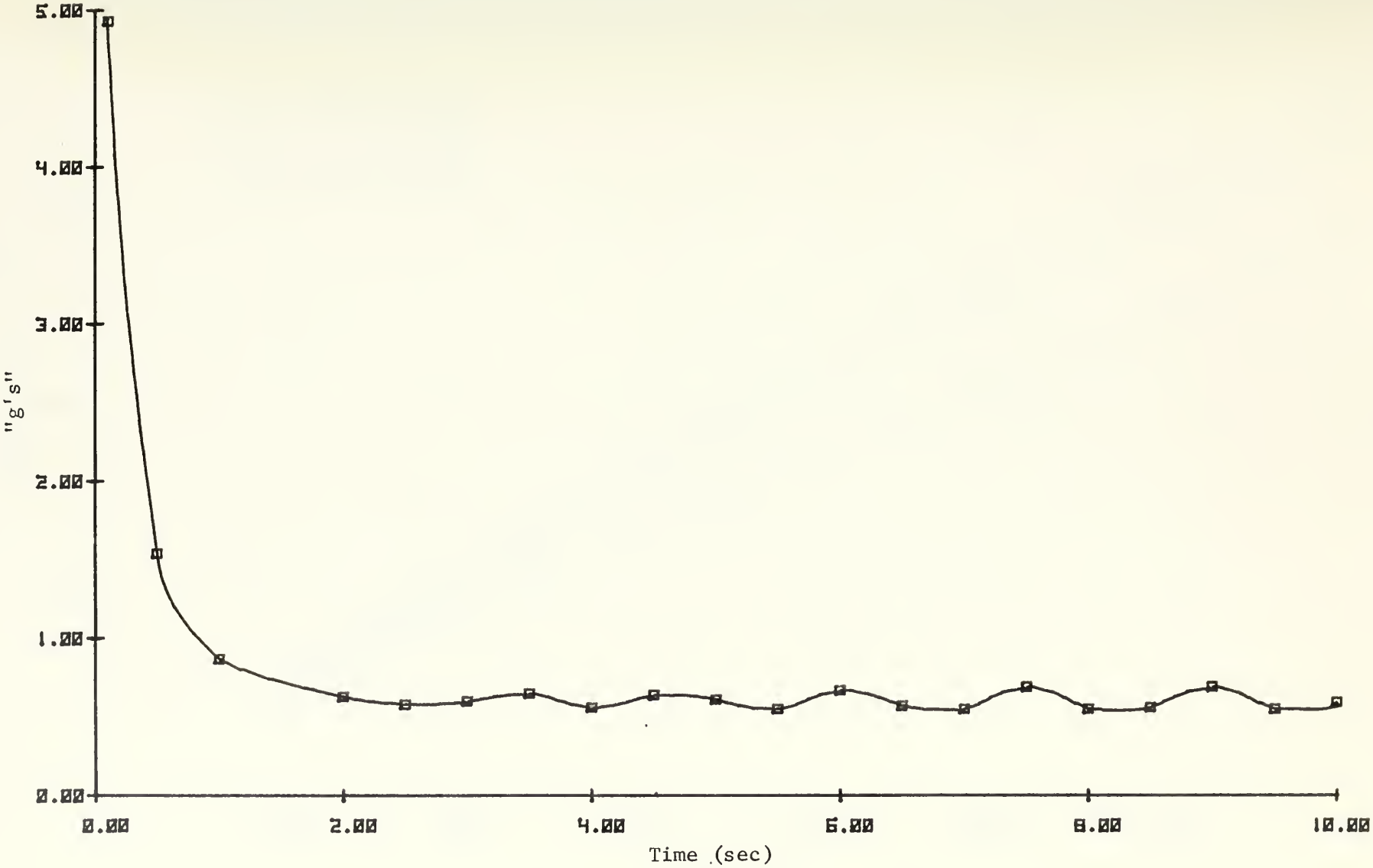

Figure 9 Linear Acceleration for Base Configuration

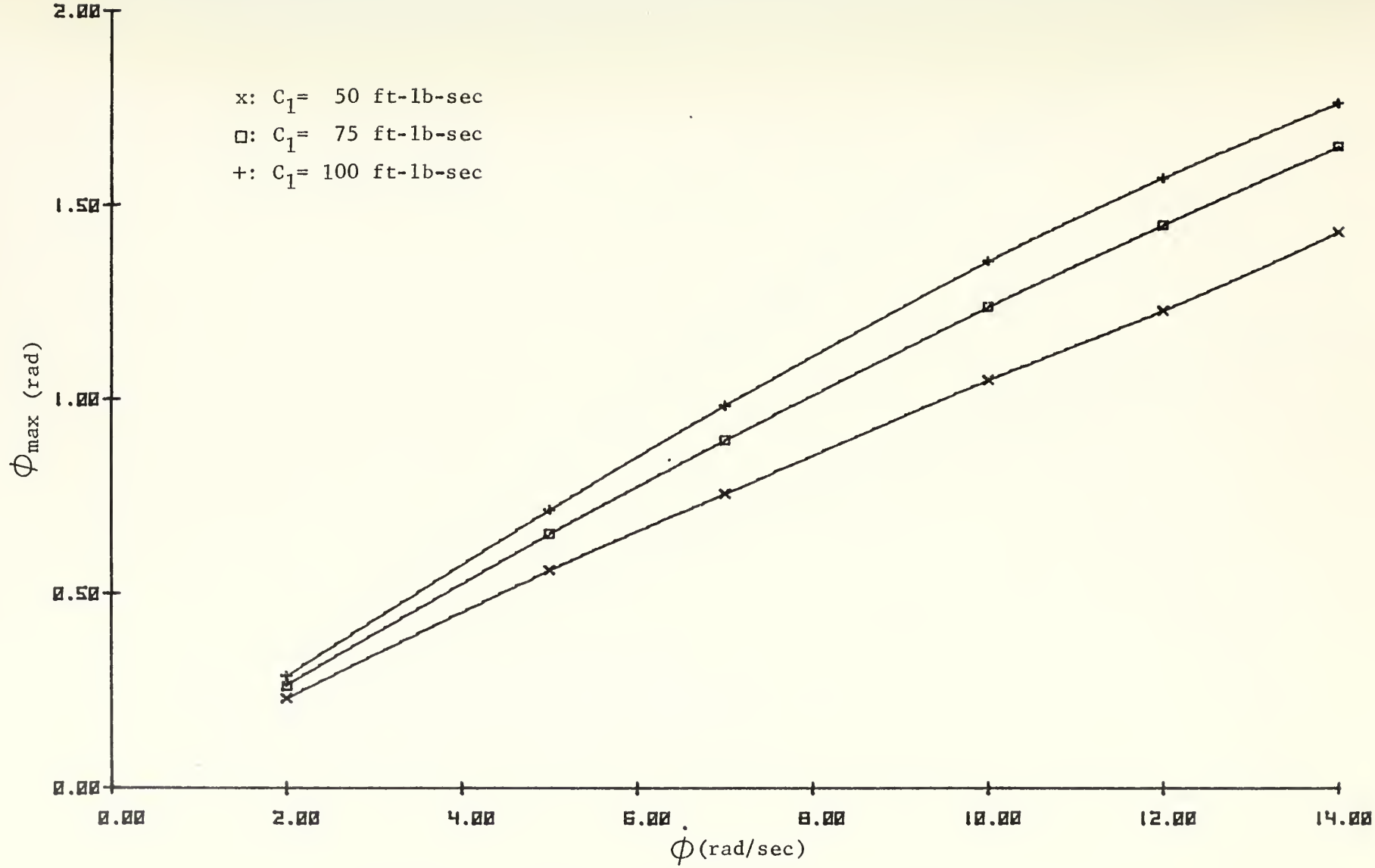

Figure 10 Effects of Damping C_1 on ϕ_{max} with C_2 Damping

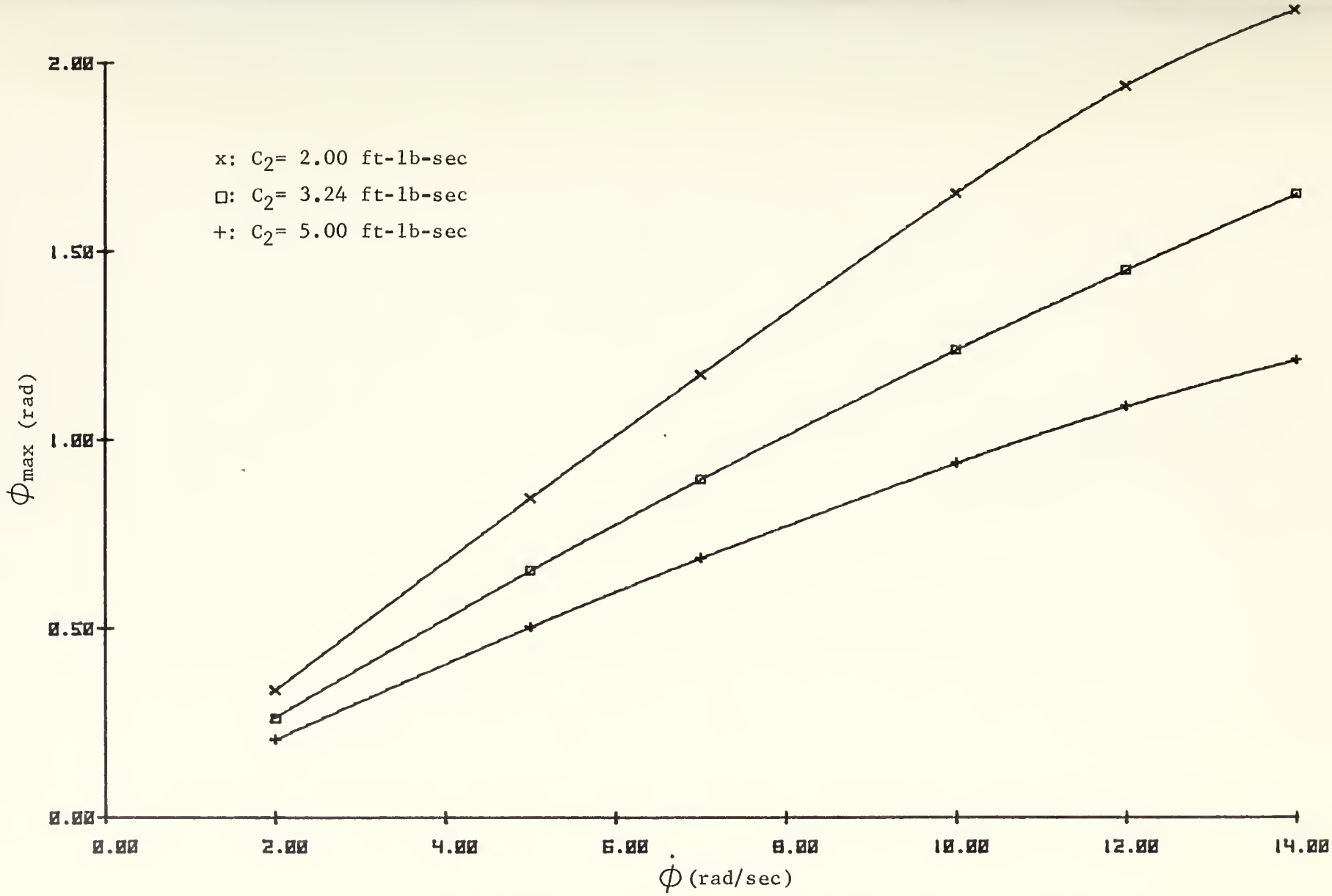

Figure 11 Effects of Damping C_2 on ϕ_{max}

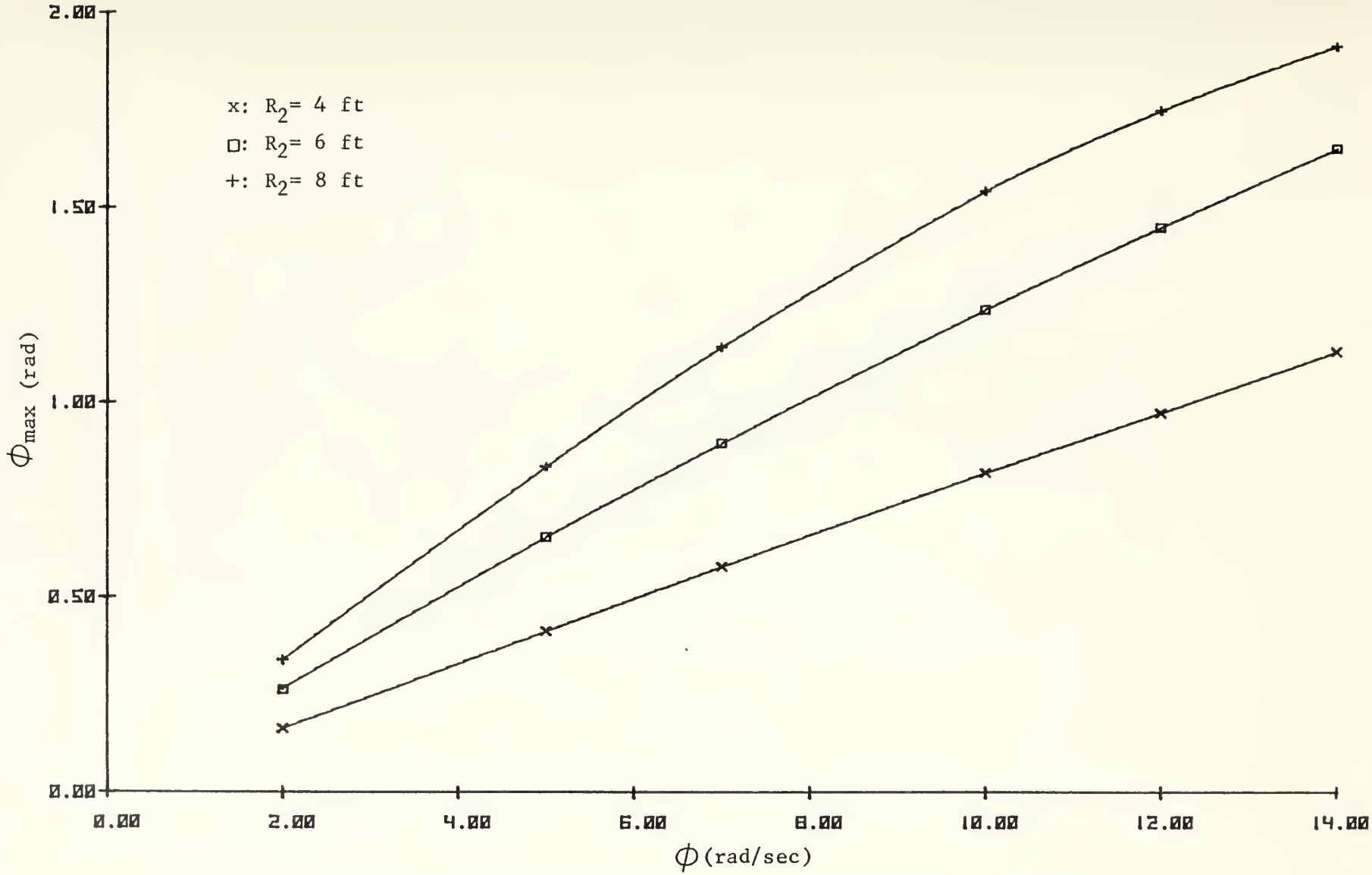

Figure 12 Effects of Rod Length R_2 on ϕ_{max} with C_1, C_2 Damping

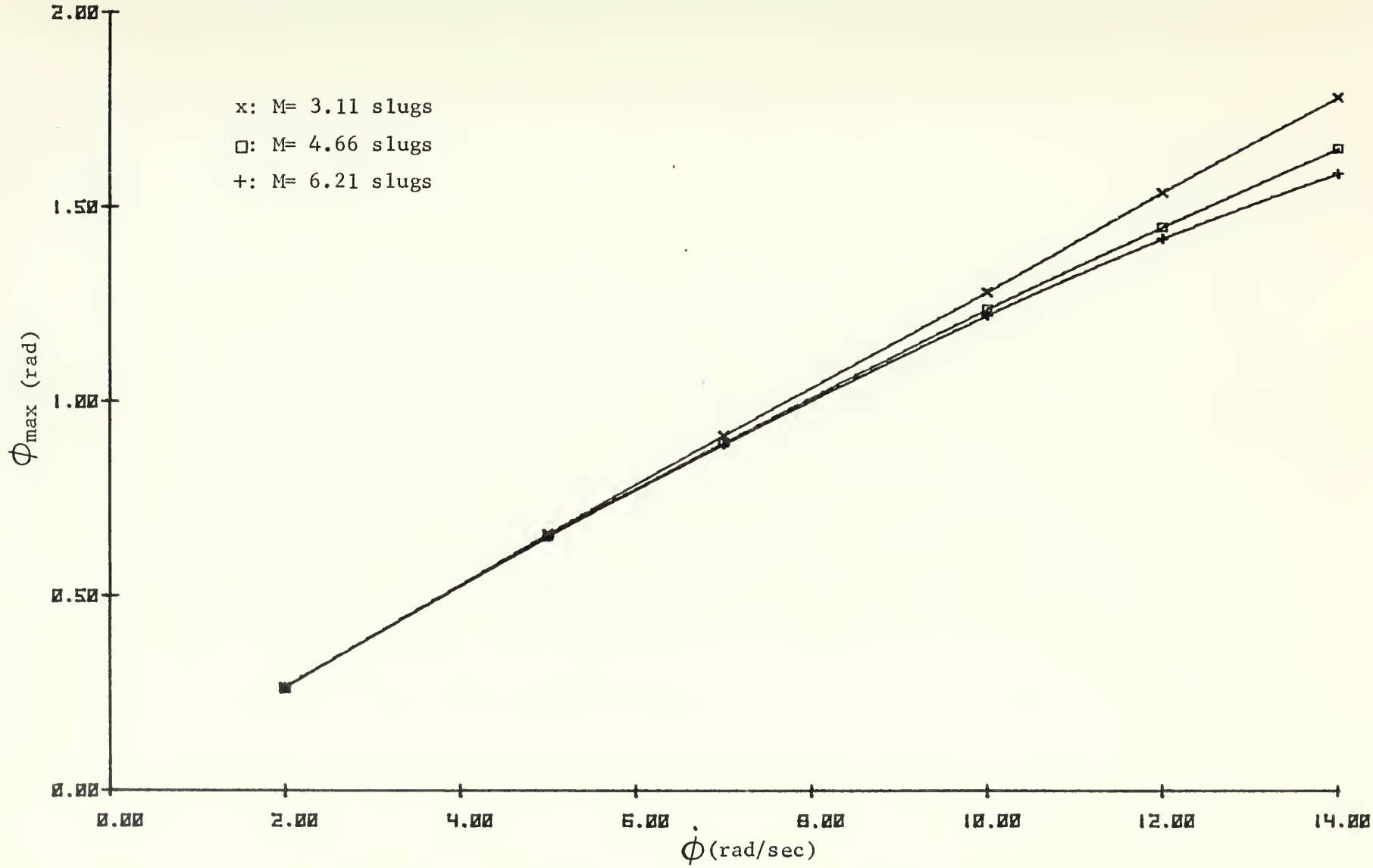

Figure 13 Effects of RPV Mass on ϕ_{max} with C_1, C_2 Damping

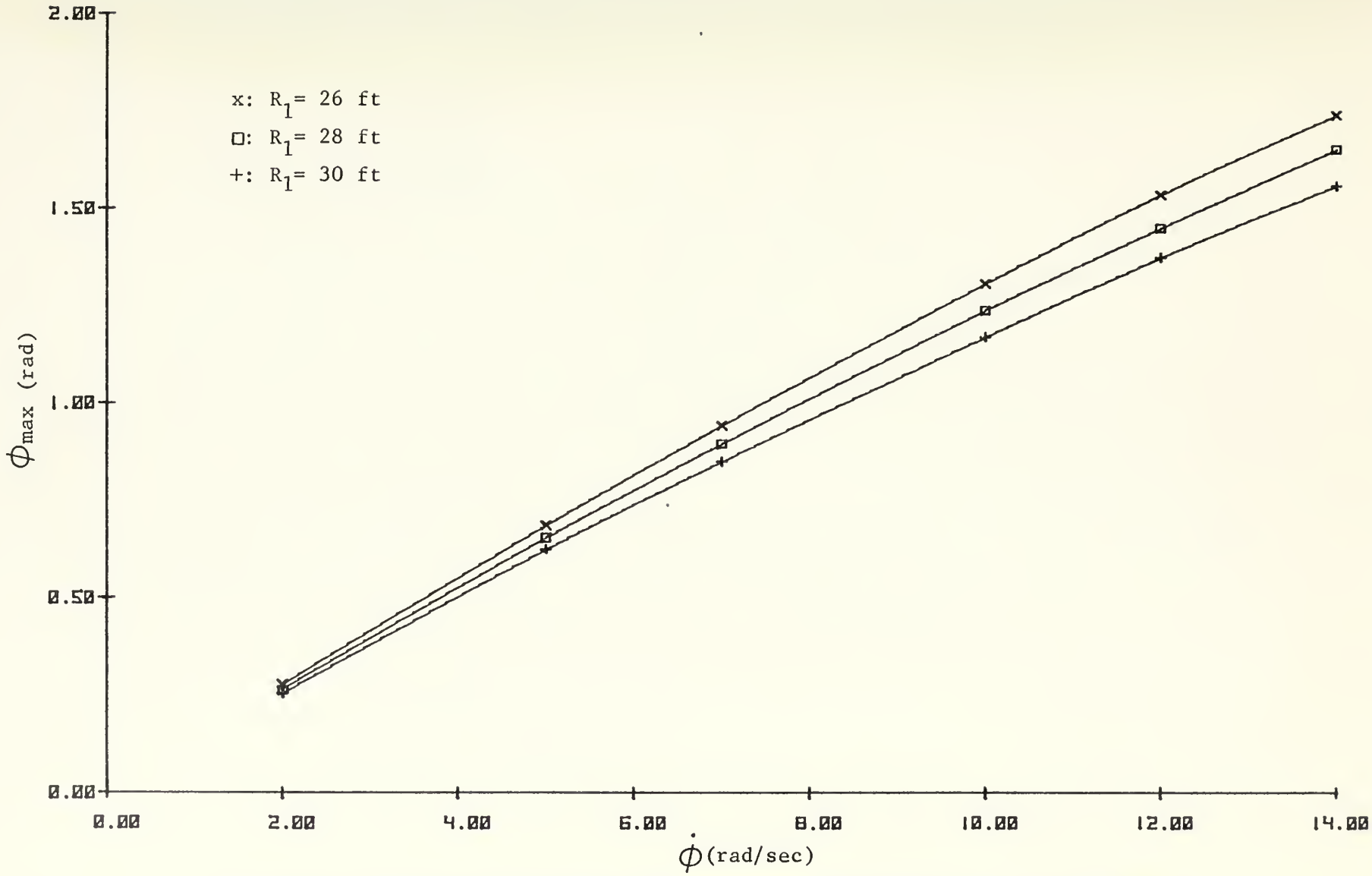

Figure 14 Effects of Horizontal Member Length R_1 on ϕ_{max} with C_1, C_2 Damping

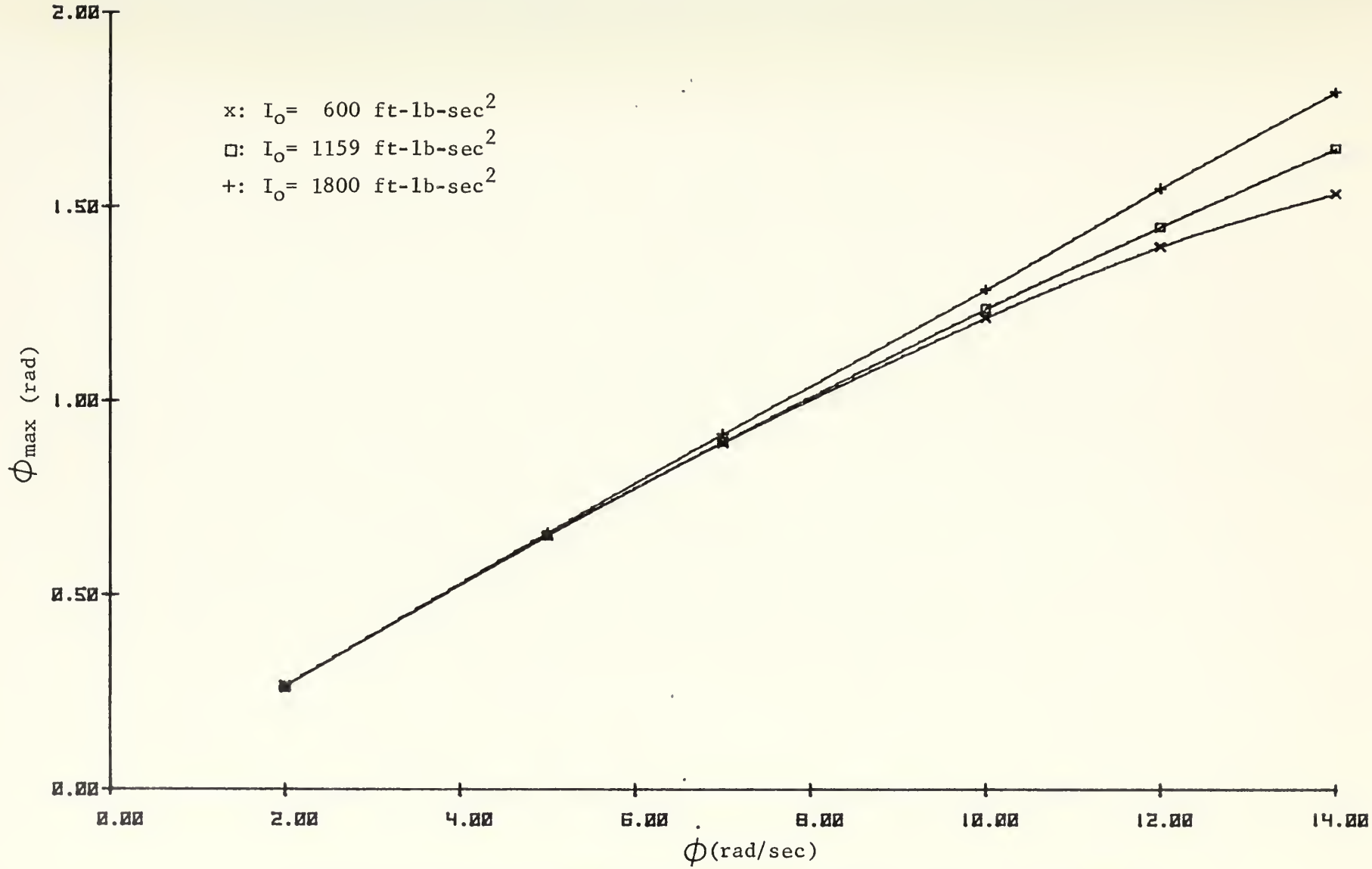

Figure 15 Effects of Moment of Inertia I_o on ϕ_{max} with C_1, C_2 Damping

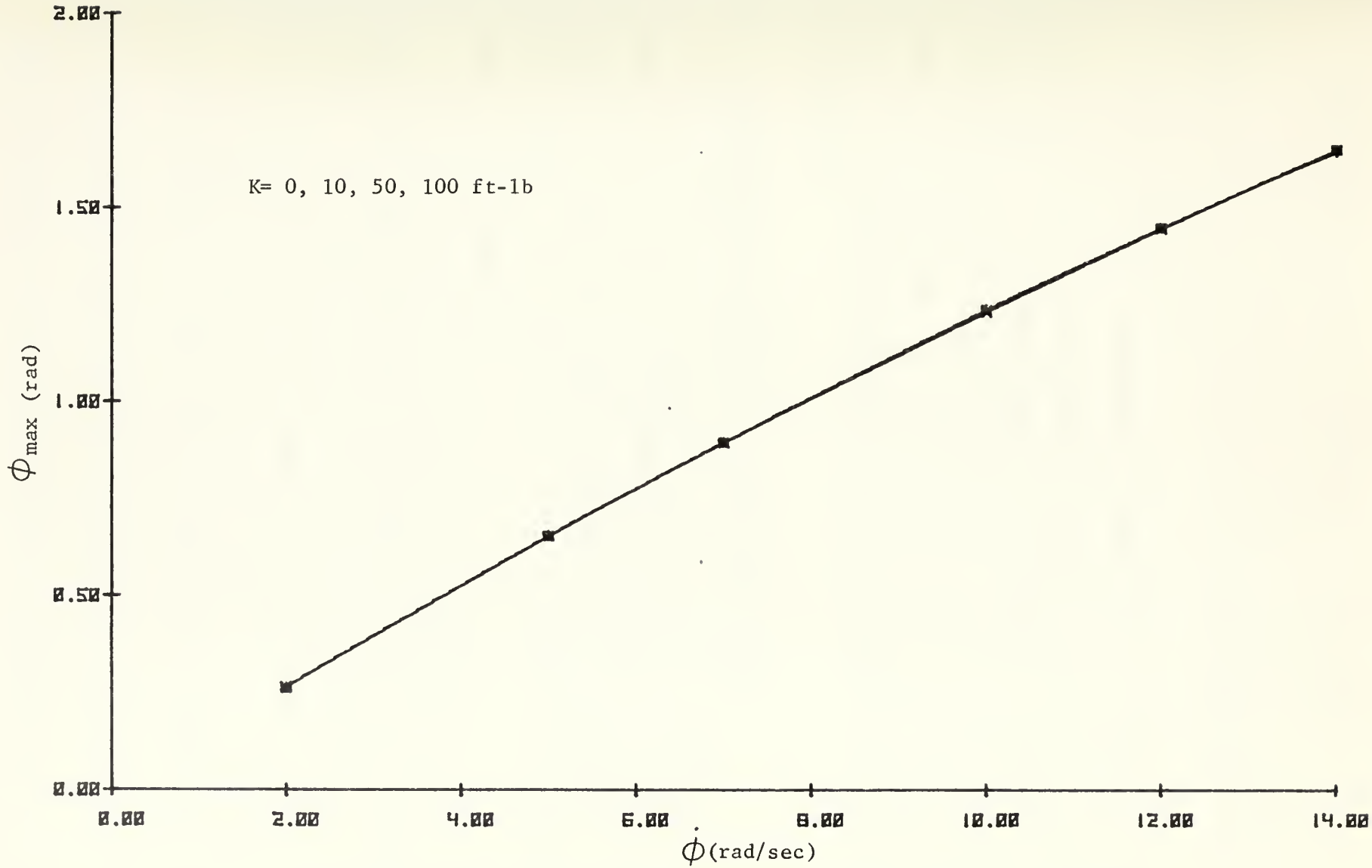

Figure 16 Effects of Spring Constant K on ϕ_{max} with C_1, C_2 Damping

The system was also sensitive to the value of C_1, but more sensitive to C_2. This, however, should not present a problem, as C_1 and C_2 will be set by the design and will not vary in operation.

The system was relatively insensitive to variations of the point along the horizontal member, R_1, where the RPV was caught. The system was also relatively insensitive to variations in the moment of inertia, I_o, of the horizontal member and the mass, M, of the RPV. The maximum displacement of ϕ was not affected at all by changes in the spring constant, K.

D. IMPLEMENTING DAMPING ON A RECOVERY CABLE

The damping desired at the pivot of the horizontal member can be readily implemented in actual construction. However, it was not readily apparent how the damping of the vertical rod, which was a cable in the actual system, could be implemented.

Two simple pendulum designs were analysed and modeled using the same techniques described to study the recovery system. The intent was to see if pivotal damping could be applied effectively to control the swing of a cable.

The first design is shown in Figure 17 and simulates a cable design for the vertical massless recovery rod that was used in the recovery system analysis. With no pivotal damping, an initial velocity was applied to M_2 to make ϕ_{2max} approach a high angle without exceeding 180 degrees.

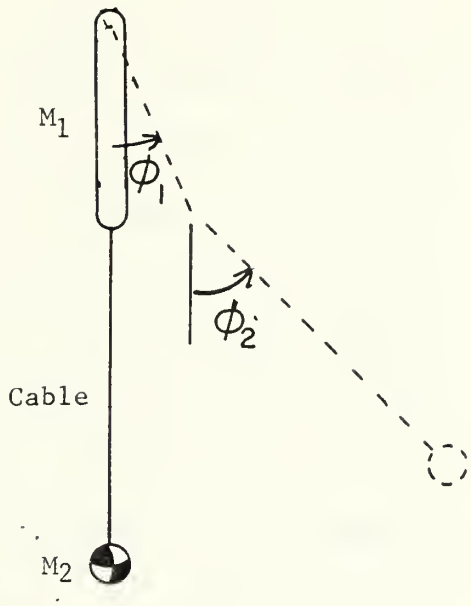

Figure 17 Pendulum Design A

Then damping was applied to the pivot of the cable support M_1 to judge its effect on reducing the magnitude of ϕ_2. The results are plotted in Figure 18. This approach of applying pivotal damping did not effectively reduce ϕ_{2max} as desired.

Another design, shown in Figure 19, was also analysed to see if it could, through pivotal damping, control the maximum magnitude of ϕ_2. Again the design simulated a cable instead of the massless recovery rod used in the analysis. A spring was used at the pivot to give M_1 a near horizontal static deflection. With no damping applied, an initial velocity was found for M_2 that caused ϕ_{2max} to approach 180 degrees. Pivotal damping was then applied to M_1 to observe its effect on the magnitude of ϕ_2. The results shown in Figure 20 indicate that pivotal damping applied to this pendulum design was also ineffective in reducing ϕ_{2max}.

While neither of these designs demonstrated effective control of ϕ_2, they by no means exhaust the possible methods of implementing damping in a cable design, and further study is possible.

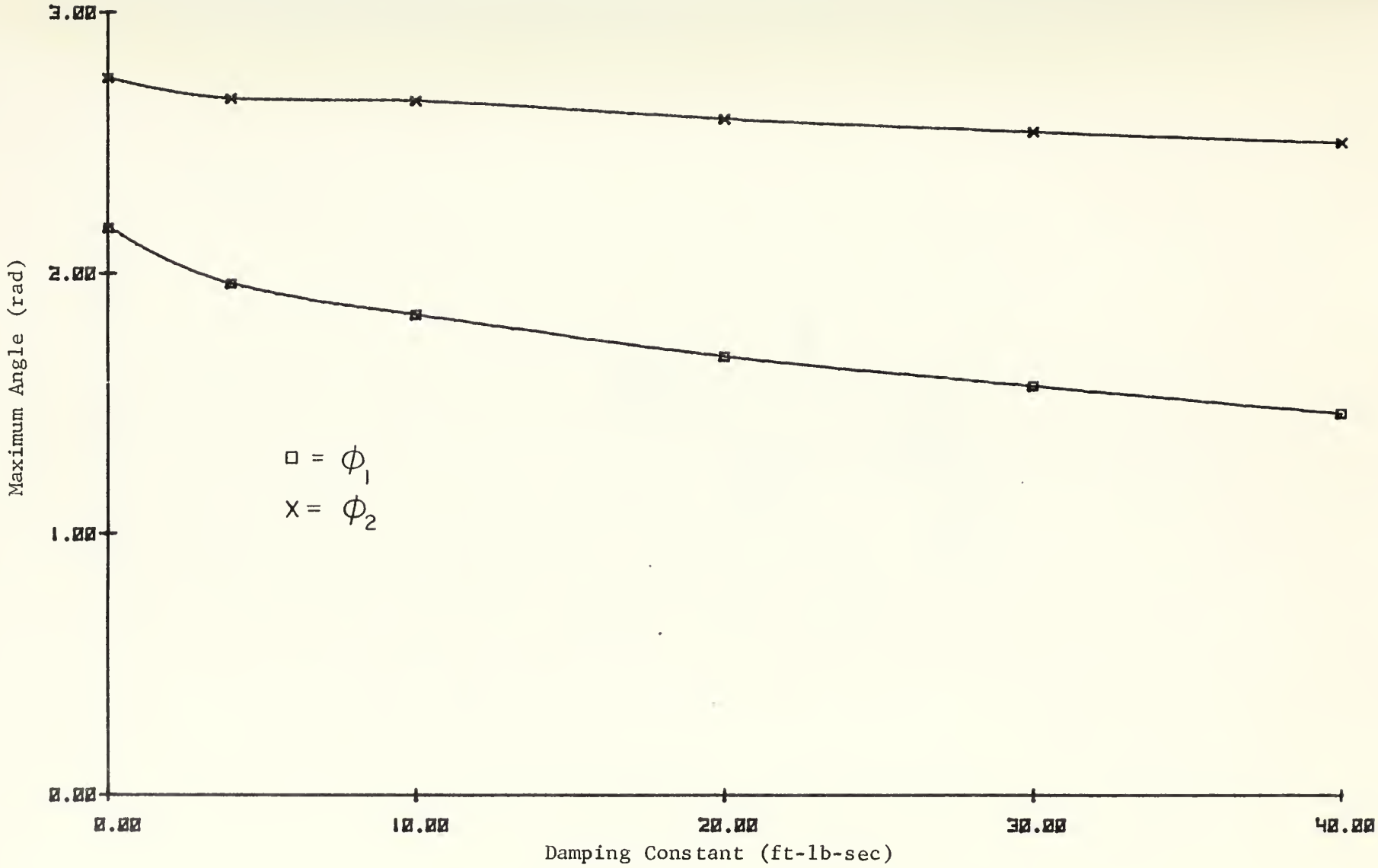

Figure 18 Results of Pendulum A Analysis

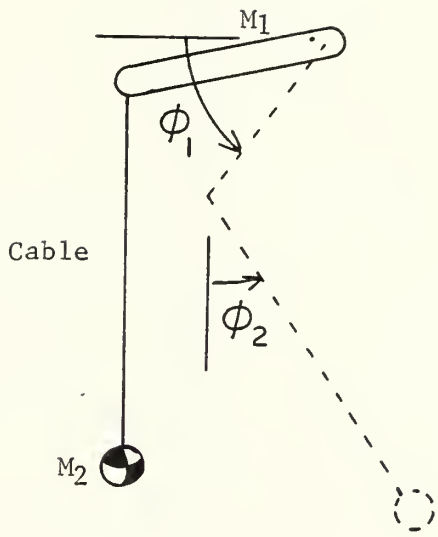

Figure 19 Pendulum Design B

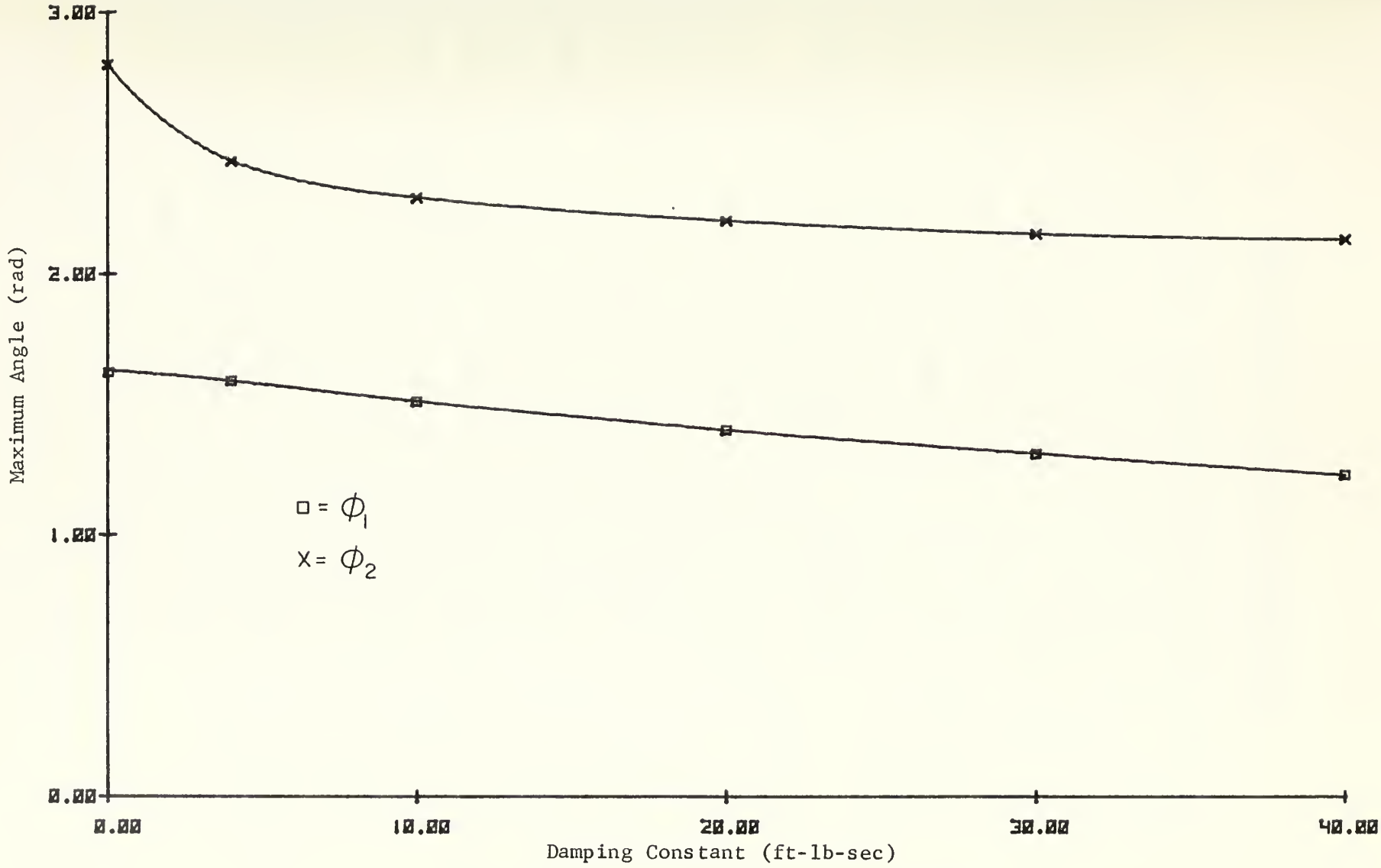

Figure 20 Results of Pendulum B Analysis

IV. CONCLUSIONS AND RECOMMENDATIONS

For the carousel recovery system to be feasible at approach speeds of 50 knots, a relatively small amount of damping was required at the pivot of the recovery rod in addition to damping at the pivot of the horizontal member. The damping at both pivots was required to prevent the maximum swing of the point mass RPV from exceeding approximately 90 degrees in the ϕ direction, the coordinate that exhibited the largest change in magnitude.

The recovery system was sensitive to the vertical height of the RPV at the time it was captured. The greater the distance, R_2, between the RPV and the horizontal member, the greater the swing of the RPV relative to the horizontal member. When selecting parameter values such as the damping constants under the most severe conditions, the RPV should be assumed to have contacted the recovery system at the maximum length of the recovery rod or cables.

The recovery system was relatively insensitive to variation in the distance the RPV was from the vertical mast when it was caught. The system was also relatively insensitive to variations in the mass of the RPV and the moment of inertia of the horizontal member.

Variations in the spring constant for the torsional spring located at the pivot of the horizontal member had little effect on the swing of the RPV. Since it was not

important to controlling the motion of the RPV, it could be removed from the design.

The magnitude of linear acceleration exhibited by the RPV, with the recovery system design that incorporated both horizontal member and recovery rod damping, was within Aquila load limits.

Based on this analysis the carousel recovery system is still viable; however, it is apparent that the system will be sensitive to approach techniques used during the recovery.

It is recommended that this analysis be continued, in order to treat the RPV as a distributed mass with its own moment of inertia and coordinate system, and caught by two recovery rods or cables, one for each wing tip, instead of one. Expanding the scope of the recovery system model would provide a more detailed analysis of the RPV's linear lateral, longitudinal and normal accelerations and hence insure that they were individually within the RPV's design limits.

It is also recommended that the effects of an RPV approaching at angles to the recovery system be investigated; this should result in increased motion in the ψ direction.

It is further recommended that continued study should be made of a means of applying damping to the swing of the vertical recovery cables.

APPENDIX

MODELING THE EQUATIONS OF MOTION USING CSMP

An application-oriented software package called the Continuous System Modeling Program (CSMP) was used to model and solve the nonlinear, cross-coupled equations of motion. CSMP is a powerful software package that can handle this type of problem routinely. In the analysis performed in this thesis two integrations using a fourth order variable integration step Runge-Kutta technique on each of the three equations of motion, Ref. 5. This sophisticated integration technique has the advantage of automatically adjusting the time increment of integration to meet the demands of the dynamic conditions of the simulation. The absolute value of the estimated integration error and the relative magnitude of the estimated error are compared with user specified error-bounds. The step size is then adjusted to meet the desired error criteria. In the analysis performed in this thesis the default value of .0001 for both the absolute and relative errors was used.

The program structure of CSMP is composed of three segments; Initial, Dynamic, and Terminal. Generally, data statements will appear in the Initial segment. In addition, calculations that are required to be performed only one time during the simulation can be conveniently placed in

this segment. The Dynamic segment is usually composed of structural statements that describe the dynamics of the system or explicitly describe a set of differential equations. The Terminal segment is the last segment in the program and is usually made up of output control statements.

The actual program used in this analysis for the undamped system will now be described. List of symbols used in the Computer Programs:

R1 - Length of horizontal member in feet

R2 - Length of recovery rod in feet

M - Mass of RPV in slugs

MIO - Moment of inertia of horizontal member in ft-lb-sec^2 about its pivot point

K - Spring constant, in ft-lb/rad, of spring at pivot of horizontal member

X5I - Initial angular velocity of the recovery rod in the ϕ direction in units of rad/sec also equal to approach velocity of RPV in ft/sec divided by R2

G - Acceleration of Gravity 32.2 ft/sec^2

X1 - θ

X2 - ϕ

X3 - ψ

X4 - $\dot{\theta}$

X5 - $\dot{\phi}$

X6 - $\dot{\psi}$

X4DOT - $\ddot{\theta}$

X5DOT - $\ddot{\phi}$

X6DOT - $\ddot{\psi}$

CO - C_1, damping constant in ft-lb-sec for the damper located at the pivot of the horizontal member

CO2 - C_2, damping constant in ft-lb-sec for the damper located where the recovery rod attaches to the horizontal member

AD - Determinant of A as defined in Section II.C.4

AD1 - Determinant of A1 as defined in Section II.C.4

AD2 - Determinant of A2 as defined in Section II.C.4

AD3 - Determinant of A3 as defined in Section II.C.4

B1 - is b_1 defined in Section II.C.4

B2 - is b_2 defined in Section II.C.4

B3 - is b_3 defined in Section II.C.4

A1 - is a_{11} defined in Section II.C.4

A2 - is a_{12} defined in Section II.C.4

A3 - is a_{13} defined in Section II.C.4

A4 - is a_{23} defined in Section II.C.4

A, B, C, D, E, F, H, L, S, T - were used to simplify program notation and are defined in the program

A description of the program shown in Figure 21, follows:

Lines 1-3: Make up the initial segment, parameters that would remain constant during the integration were assigned here.

Lines 4-34: Make up the Dynamic segment.

Lines 5-13: Simplifying notation.

```
INITIAL
 CONSTANT R1=28.0,R2=9.0,M=4.66,MIO=550.000,K=50.00,X5I=7.000,G=32.2
T=R1/R2
DYNAMIC
A=SIN(X2)
B=COS(X2)
C=SIN(X3)
D=COS(X3)
E=SIN(2.0*X2)
F=SIN(2.0*X3)
H=COS(2.0*X3)
L=SIN(X1)
S=COS(X1)
A1=MIO/(M*R2**2)+(T-C)**2+D**2*A**2
A2=A*(1.0-T*C)
A3=B*(T*D-.5*F)
A4=D**2
AD=A2**2*A4-A1*A4+A3**2
AD1=A2*B3*A4-B1*A4+B2*A3
AD2=A2*(B1*A4-B2*A3)-B3*(A1*A4-A3**2)
AD3=A2**2*B2-B2*A1+B1*A3-B3*A3*A2
B1=T*A*D*X6**2+A*(T*D-.5*F)*X5**2-(F*B**2-2.0*T*D)*X4*X6-E*D**2*X4*X5...
-(1.0-H-2.0*T*C)*B*X6*X5-(K*X1)/(M*R2**2)
B2=.5*D**2*E*X4**2+B*(1.0+H)*X4*X6+F*X6*X5-G*A*D/R2
B3=(.5*F*B**2-T*D)*X4**2-.5*F*X5**2-B*(1.0+H)*X4*X5-G*B*C/R2
X4DOT=AD1/AD
X5DOT=AD3/AD
X6DOT=AD2/AD
X4=INTGRL(0.0,X4DOT)
X5=INTGRL(X5I,X5DOT)
X6=INTGRL(0.0,X6DOT)
X1=INTGRL(0.0,X4)
X2=INTGRL(0.0,X5)
X3=INTGRL(0.0,X6)
TERMINAL
TIMER FINTIM=30.0
* THESIS WORK 32
PRINT X1,X2,X3,X4,X5,X6,X4DOT,X5DOT,X6DOT,A1,A2,A3,A4,AD,B1,B2,B3,...
AD1,AD2,AD3,T
END
STOP
```

Figure 21 Computer Program

Lines 14-28: The algebra used to solve for $\ddot{\theta}$, $\ddot{\phi}$ and $\ddot{\psi}$ prior to integration as described in Section II.C.4.

Lines 29-31: Perform the first integration from angular accelerations to angular velocities.

Lines 32-34: Perform the second integration from angular velocities to angular position.

Lines 35-41: Make up the Terminal segment.

Line 36: Limits the time period that will be modeled.

Lines 38-39: Prints output as a function of time.

When damping was added to the horizontal member the only changes that occurred to the program were the following:

Line 2: add <u>,CO = 75</u>

Line 23: add <u>-CO * X4</u>.

When damping was also added to the recovery rod the additional changes that occurred to the program were as follows:

Line 2: add <u>,CO2 = 3.24</u>

Line 24: add <u>-CO2 * X5</u>

LIST OF REFERENCES

1. ARMY Aviation RDT&E Plan, U.S. Army Aviation Systems Command, July 1975.

2. Mini-RPV Recovery System Conceptual Study, USA-AMRDL-TR-77-24, August 1977.

3. Meirovitch, Leonard, Methods of Analytical Dynamics, McGraw-Hill Book Company, New York, p. 72-79, 88-91, 1970.

4. Kreyszig, Erwin, Advanced Engineering Mathematics, John Wiley and Sons, Inc., New York, 1972.

5. Speckhart, Frank H. and Green, Walter L., A Guide to Using CSMP, Prentice-Hall, Inc., Englewood Cliffs, New Jersey, 1976.

INITIAL DISTRIBUTION LIST

		No. Copies
1.	Defense Documentation Center Cameron Station Alexandria, Virginia 22314	2
2.	Library, Code 0142 Naval Postgraduate School Monterey, California 93940	2
3.	Department Chairman, Code 67 Department of Aeronautics Naval Postgraduate School Monterey, California 93940	1
4.	Professor L. V. Schmidt, Code 67Sx Department of Aeronautics Naval Postgraduate School Monterey, California 93940	1
5.	J. K. Marstiller AVRADCOM ATTN: DRDAV-RP P. O. Box 209 St. Louis, Missouri 63166	1
6.	Cpt. Russell N. Robinson 1164 Spruance Road Monterey, California 93940	1
7.	Command & General Staff College ATTN: Educational Advisor Room 123, Bell Hall Fort Leavenworth, Kansas 66027	1

Thesis
R6426
c.1
Robinson
174002
Dynamic analysis of
a carousel remotely
piloted vehicle re-
covery system.

Thesis
R6426
c.1
Robinson
174002
Dynamic analysis of
a carousel remotely
piloted vehicle re-
covery system.

thesR6426
Dynamic analysis of a carousel remotely
3 2768 001 94910 0
DUDLEY KNOX LIBRARY